ToF-SIMS, XPS and DFT Study of the Adsorption of 2-mercaptobenzothiazole on Copper in Neutral Aqueous Solution and Corrosion Protection in Chloride Solution

Eléa Vernack, Sandrine Zanna, Antoine Seyeux, Dominique Costa, Fatah Chiter, Philippe Tingaut, Philippe Marcus

ToF-SIMS, XPS and DFT Study of the Adsorption of 2-mercaptobenzothiazole on Copper in Neutral Aqueous Solution and Corrosion Protection in Chloride Solution

Eléa Vernack, Sandrine Zanna, Antoine Seyeux, Dominique Costa, Fatah Chiter, Philippe Tingaut, Philippe Marcus

PII: S0010-938X(22)00772-7

DOI: https://doi.org/10.1016/j.corsci.2022.110854

Reference: CS110854

To appear in: *Corrosion Science*

Received date: 3 September 2022
Revised date: 15 November 2022
Accepted date: 19 November 2022

Please cite this article as: Eléa Vernack, Sandrine Zanna, Antoine Seyeux, Dominique Costa, Fatah Chiter, Philippe Tingaut and Philippe Marcus, ToF-SIMS, XPS and DFT Study of the Adsorption of 2-mercaptobenzothiazole on Copper in Neutral Aqueous Solution and Corrosion Protection in Chloride Solution, *Corrosion Science,* (2022) doi:https://doi.org/10.1016/j.corsci.2022.110854

ToF-SIMS, XPS and DFT Study of the adsorption of 2-mercaptobenzothiazole on copper in neutral aqueous solution and corrosion protection in chloride solution

Eléa Vernack[a,b], Sandrine Zanna[a],* Antoine Seyeux[a], Dominique Costa[a],* Fatah Chiter[a], Philippe Tingaut[b] and Philippe Marcus[a],*

[a]PSL Research University, Chimie ParisTech-CNRS, Institut de Recherche de Chimie Paris (IRCP), Research Group Physical Chemistry of Surfaces, 75005 Paris, France

[b]SOCOMORE, 56000 Vannes, France

*corresponding authors:

Dominique.costa@chimiparistech.psl.eu Sandrine.zanna@chimieparistech.psl.eu
philippe.marcus@chimieparistech.psl.eu

Abstract

X-ray photoelectron spectroscopy (XPS) and time-of-flight secondary ions mass spectrometry (ToF-SIMS) analyses were performed to characterize the interaction of Cu with mercaptobenzothiazole (MBT) in aqueous solution for 1 h and 24 h in absence and presence of NaCl. The fingerprints of the molecules are identified with XPS (S, N and C signals). The analysis of the Cu 2p core level and Auger Cu peaks allow us to show that the Cu metal is covered by a Cu_2O oxide layer whose thickness increases with exposure time in the absence of MBT. It is found that MBT forms multilayers on Cu oxide and inhibits the oxide layer growth. The XPS data are consistent with MBT adsorbed on oxide in multilayers, with a small fraction adsorbed on metallic Cu. These interactions are then further characterized using ToF-SIMS. The results suggest adsorption of the MBT molecules in a strongly bonded layer through both S atoms of the organic molecule oriented towards the surface, covered by a weakly bonded multilayer. Quantitative treatments of XPS intensities allows us to evaluate a layer thickness of 23 Å and 32 Å after 1 h and 24 h, respectively. Co-adsorbed water is also identified. The presence of water in the organic layer (ratio H_2O/MBT = 0.28) may explain the orientation of the molecules with S directed towards the surface and N interacting through H bonds with water molecules, as suggested by complementary DFT calculations. The

adsorption of MBT is similar in presence of NaCl and in pure water, and also inhibits the oxide growth. In addition, MBT adsorption inhibits the adsorption of Cl on the Cu surface. Inductively Coupled Plasma Optical Emission Spectrophotometry (ICP OES) experiments demonstrate that MBT adsorption inhibits Cu dissolution, even after 20 days immersion in NaCl. Thus, we demonstrated that MBT, by adsorbing and forming a full monolayer at the Cu surface, inhibits further oxide growth, Cl adsorption and copper dissolution in NaCl.

GRAPHICAL ABSTRACT

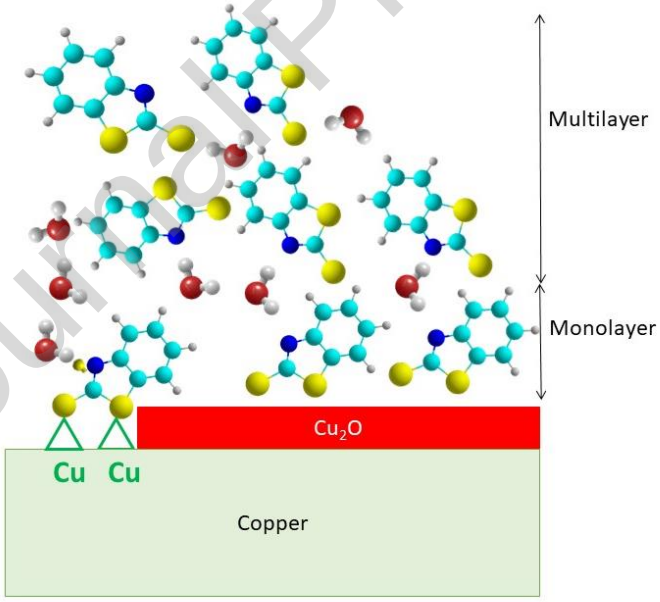

Introduction

2-mercaptobenzothiazole (MBT) is an organic corrosion inhibitor commonly used in various industrial sectors. MBT is classified as a predominantly cathodic mixed inhibitor. Used as a corrosion inhibitor for copper [1–4], it is also used in coatings for aluminium alloys [5–7], especially alloys containing copper. Although the requirement of the formation of a full adsorbed layer at the surface is widely accepted, the mechanisms of adsorption are still debated.

Due to its chemical structure, MBT exhibits a tautomeric equilibrium and can adopt either a thiol or a thione form (**Figure** 1). Several studies have shown that in the solid state the thione form of MBT is predominant [8]. The pKa of 7 of this molecule indicates that in pure water, it can be deprotonated in its thiolate form [9]. MBT contains heteroatoms, nitrogen and sulfur, involved in the adsorption on surfaces. In the literature, different MBT layer thicknesses are reported, generally attributed to different modes of adsorption. Monolayers were identified on Cu, in agreement with the unambiguously admitted fact that thiol molecules adsorb in a dense layer at this surface [10–14]. In these papers, the reported organic layer thickness was 1 to 2 nm. Chadwick and Hashemi investigated the mechanism of MBT film formation on a metallic copper surface [14]. Their study was carried out for solutions containing NaCl at different pH values [14]. According to the authors, the endocyclic sulfur is not involved in the adsorption mode of MBT on copper and MBT would be adsorbed only via the sulfur of its thiol function. Finšgar *et al* also studied the adsorption of MBT to a copper surface in chloride medium [12]. According to the analyses, only the exocyclic sulfur (exo S) atom and the nitrogen atom are involved in the adsorption mode, rather than the endocyclic sulfur (endo S). They reported that the molecule is adsorbed in bridge *via* these two atoms and binds to the Cu(I) present on the surface. Woods *et al* reported that MBT forms a monolayer on copper, silver and gold surfaces and adsorbs *via* exocyclic sulfur [13]. Lee *et al* studied the adsorption of MBT on silver [15] and Shervedani *et al* studied the adsorption of MBT on gold [16]. They reported that the endocyclic sulfur of MBT is also involved in the mode of adsorption, which would cause the molecule to tilt on the surface.

Recently, Wu *et al* reported a detailed characterization of the first monolayer of MBT on Cu from the gas phase, followed by subsequent adsorption of molecules forming multilayers above the chemically adsorbed monolayer [10,17]. To go further towards realistic conditions, water vapor was then introduced on Cu with a pre-adsorbed MBT multilayer [18]. Water displaces the molecules in the multilayers, but not the monolayer adsorbed on Cu. Thus, model studies evidence the affinity of MBT to the Cu surface, and suggest that the adsorption is competitive with regards to water adsorption.

Regarding corrosion resistance, most experiments are performed in aqueous solution, where the copper surface is oxidized. Thus, the question of MBT adsorption on an oxidized Cu surface was also addressed in the literature. Quartz cristal microbalance was used by Ramírez-Cano *et al* to estimate the coverage of

MBT on the surface, and a value of 0.5 monolayer at 10^{-1} M in water was found [19]. An ultrathin layer thickness was measured *in situ* with ellipsometry by Kuznetsov *et al*, equivalent to a thickness of 0.3 nm, or to a partial coverage [20]. XPS studies by Tan *et al* [11] and Finšgar *et al* concluded to adsorption of a monolayer, with a thickness of 1.0-1.5 nm [12]. Other works however report the formation of multilayers of Cu^{I}-MBT complexes, of thicknesses 2 to 9 nm, depending of the experimental conditions [21] [22]. These multilayers are formed after dissolution and redeposition of a Cu^{I}-MBT complex. However, even in the presence of deposited complex multilayers, a full adsorbed MBT layer is formed at the surface, which surface state and molecule-surface interaction are still not fully characterized.

A gas phase study of adsorption of MBT on 3D-oxidized copper concluded to the formation of MBT multilayers on Cu_2O [17]. Therefore, on Cu oxide as on Cu metal, MBT adsorbs and forms multilayers even without complexes redeposition. This study in gas phase did not conclude into a favored adsorption mode of the molecule, as no signal specific of S-Cu^{ox} or N-Cu^{ox} could be identified. To the best of our knowledge, the MBT-Cuox interface and adsorption mode was studied in only one theoretical paper, that concluded in adsorption through S exo and N [23].

In addition to molecule deposition, it was reported that thiols might reduce the copper oxide layer and induce surface roughness, that would result in a denser thiol layer [24]. Aromatic thiols inhibit the growth of oxide layer on Cu immersed in alkaline solution, the S 2p binding energy recorded being 162.3 ±0.1 eV, typical of thiol-Cu interaction [25]. The same phenomenon was observed for azoles, as XPS analyses show that the Cu_2O layer formed during 10 min air exposure is partially consumed during subsequent immersion in BTAH aqueous solution [26]. These results are in agreement with gas phase experiments which show that on 2D oxide, MBT displaces adsorbed oxygen on Cu [17] .

The complementarity of ToF-SIMS and XPS is known to gain in precision to determine the orientation of molecules adsorbed on a surface. The combination of these two methods was used recently by Finšgar to study the adsorption of azole on oxidized copper in NaCl [27] and of MBT on an Al alloy [5]. For Cu, the author concluded to the formation of a layer of azoles, above which a layer of Cu-azole complexes was re-deposited after Cu dissolution. On Al alloy, MBT adsorbed in patches on the Al surface.

Here we complete the campaign of gas phase and model studies, with the immersion of copper in aqueous solution containing MBT (without and with NaCl). The XPS data are analysed thanks to the previous works performed on model systems, and other data in the literature. In addition to XPS, ToF-SIMS analyses are performed on samples immersed in water and water + MBT, that help for understanding the molecule-surface interaction and molecule orientation. DFT calculations are performed and contribute to the interpretation of experimental data. Finally, the corrosion resistance in chloride solution is tested

through ICP-OES experiments, and correlated with the surface composition and Cl content as measured with XPS.

Materials and methods

I - Sample preparation

Rolled copper of 99.99% purity purchased from Goodfellow® was used. Samples were cut in 1 x 1 cm² square sheets and had a thickness of 1 mm. Cu samples were then first mechanically polished with SiC paper (1200, 2400 and 4000) under water followed by manual polishing down to 0.25 µm using diamond suspension until a mirror-like finish is reached. Finally, samples were ultrasonically cleaned for 2 min in ethanol and deionized water (18.2 Mohm.cm) and dried with filtered air. MBT (2-mercaptobenzothiazole) 99% powder from Sigma-Aldrich® was used. MBT molecules are aromatic heterocycles as shown in **Figure 1**. MBT molecules were first analyzed in powder form. They were deposited on carbon tape before analysis.

Cu immersion in solution :

Cu samples were immersed in a solution of ultra-pure water containing 1.0 mmol. L^{-1} of MBT molecule for 1 hour and 24 h at room temperature (20 ± 2 ° C). This concentration was selected because it is the maximum solubility of MBT in our media. The immersion volume is set at 200 mL for all the solutions. The same procedure was applied in NaCl 0.05 mol/L, prepared from ultra-pure water, to which 1.0 mmol.L^{-1} MBT was added. After immersion, the samples are rinsed with ultra-pure water and dried with compressed air before being analyzed.

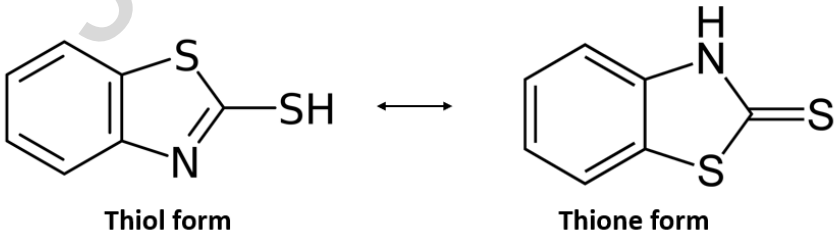

Figure 1 : Schematic representation of the MBT molecule

II - Experimental methods

Surface characterization was done by X-ray photoelectron spectroscopy (XPS) and Time-of-Flight Secondary Ion Mass Spectrometry (ToF-SIMS).

XPS analysis was performed with a Thermo Electron Escalab 250 spectrometer using a monochromatic Al Kα X-ray source (hν = 1486.6 eV) at a residual pressure below 10^{-9} mbar. The take-off angle was 90° and the analyzed area was a 500 µm diameter disk. High resolution core level spectra were recorded with a pass energy of 20 eV at a step size of 0.1 eV for C 1s, O 1s, Cu 2p, N 1s and S 2p as well as Auger spectra (Cu LMN). The AvantageTM software (Thermo ElectronCorp.) was used to fit the spectra with a Shirley type background and Lorentzian/Gaussian 30/70 peak shape for oxides. The CasaXPS processing software was also used for the fitting of Cu LMN Auger spectra.

The MBT powder was fixed on a carbon tape. Because of its insulating character, we used charge compensation to perform the analysis (in the absence of charge compensation the peaks are shifted and distorted). After charge correction, the peaks are symmetric but wide. In order to calibrate all the spectra and to compare them with each other, the energy of the C-C bond is used as a reference and fixed at 285.0 eV [28].

Quantitative treatment of the XPS intensities:

To calculate the thickness of the native oxide (d) on the polished sample, we estimated that all the Cu(I) detected on the surface was from the oxide. Assuming that the oxide layer is uniform, the following equations are applied:

$$I_{Cu\ Auger}^{Oxide} = K\ \lambda_{Cu\ Auger}^{Oxide} Y_{Cu}\ T_{Cu\ Auger}\ D_{Cu}^{Oxide} sin\theta\ \left[1 - \exp\left(\frac{-d}{\lambda_{Cu\ Auger}^{Oxide} sin\theta}\right)\right] \quad (1)$$

$$I_{Cu\ Auger}^{Metal} = K\ \lambda_{Cu\ Auger}^{Metal}\ Y_{Cu}\ T_{Cu\ Auger}\ D_{Cu}^{Metal}\ \ sin\theta \exp\left(\frac{-d}{\lambda_{Cu\ Auger}^{Oxide} sin\theta}\right) \quad (2)$$

the factor $\exp\left(\frac{-d}{\lambda_{Cu\ Auger}^{Oxide} sin\theta}\right)$ accounts for the attenuation of the metal signal by the oxide layer.

- K is a constant including the characteristic of the equipment, the analyzed surface area and the photons flux
- λ is the inelastic mean free path, θ is the take-off angle of photoelectrons. For this study, the inelastic mean free path was estimated from the Tanuma, Powell, and Penn method (TPP-2M)[29]
- Y_{Cu} is the Auger yield factor of Cu. We deduced the value from a reference sample (a metallic Cu sample).

- T is the transmission factor of the analyzer
- D_M^i is the density of element M in the matrix *i*.
- θ is the take-off angle of photoelectrons (in this work, θ = 90°, sin θ = 1)
- *I* is the intensity of the Auger peak

All numerical values are reported in SI-I section, Table SI-1.

Thanks to these two equations, we can calculate d by:

$$d = \lambda_{Cu\ Auger}^{Oxide} sin\theta \ln\left(1 + \frac{I_{Cu\ Auger}^{Oxide} \lambda_{Cu\ Auger}^{Metal} D_{Cu}^{Metal}}{I_{Cu\ Auger}^{Metal} \lambda_{Cu\ Auger}^{Oxide} D_{Cu}^{Oxide}}\right) (3)$$

To estimate the thickness of the molecular layer (noted d'), we assumed, as a first approximation, that the layer of MBT prevents the further growth of the oxide in water. The oxide would therefore keep the same thickness (noted d), i.e., the thickness of the native oxide on the polished sample (calculated by the previous method). Once the oxide layer thickness, d, is calculated, it is possible to calculate the organic layer thickness, d'. Assuming that the layer of MBT is uniform, we can use the following equations:

$$I_{Cu\ (0)Auger}^{Metal} = K\ \lambda_{Cu\ Auger}^{Cu} Y_{Cu}\ T_{Cu\ Auger}\ D_{Cu}^{Cu} sin\theta \exp\left(\frac{-d}{\lambda_{Cu\ Auger}^{Oxide} sin\theta}\right) \exp\left(\frac{-d\prime}{\lambda_{Cu\ Auger}^{MBT} sin\theta}\right) (4)$$

$$I_S^{MBT} = K\ \lambda_S^{MBT} \sigma_S\ T_S\ D_S^{MBT} sin\theta\ \left[1 - \exp\left(\frac{-d\prime}{\lambda_S^{MBT} sin\theta}\right)\right] (5)$$

d' is thus calculated from the I_S/I_{Cu} intensity ratio.

σ_S is the photoionization cross section of Sulfur.

In the case where the MBT layer is not uniform in density, it is possible to consider two MBT layers, an inner layer 1 and an outer layer 2. Then, the equation (5) becomes :

$I_S^{MBT} = K\ \lambda_S^{MBT} \sigma_S\ T_S\ sin\theta\ \{D_S^{MBT-1}\ \left[1 - \exp\left(\frac{-d1}{\lambda_S^{MBT} sin\theta}\right)\right] \exp\left(\frac{-d2}{\lambda_S^{MBT} sin\theta}\right) + D_S^{MBT-2}\ \left[1 - \exp\left(\frac{-d2}{\lambda_S^{MBT} sin\theta}\right)\right]\}$ (5'), where d1 is the thickness of the MBT layer 1, of density D_S^{MBT-1}, and d2 the thickness of MBT layer 2, of density D_S^{MBT-2}, with d1+d2 = d'

A ToF-SIMS V spectrometer (Ion ToF GmbH) operating at 10^{-9} mbar vacuum was used to record mass spectra and in-depth profiles. Mass spectra were obtained using a pulsed 25 keV Bi^+ primary ion source (LMIG) delivering a 1.2 pA current and rastering an area of 20 × 20 μm^2 for MBT powders analyses and

an area of 500 × 500 μm^2 for Cu samples. The in-depth profiles were obtained using a dual beam mode: a pulsed 25 keV Bi^+ primary ion source (LMIG) as the analysis beam delivering a 1.2 pA current and rastering an area of 100 × 100 μm^2, and a 500 eV Cs^+ ion beam as the sputtering beam delivering a 20 nA current and rastering an area of 500 × 500 μm^2. Profile acquisitions were performed in negative ion mode since it provides higher sensitivity for oxides. Data acquisition and post-processing analysis were performed using the Ion-Spec software.

The ToF-SIMS data have been obtained in High Current BUNCHED mode (IONTOF labelling) providing the highest mass resolution of the IONTOF ToF-SIMS5 spectrometer.

The measurements included in the paper have been obtained with a mass resolution of M/ΔM around 9000 and a spectrum calibration using at least 5 peaks spreading over the full mass range of the spectrum. With the resolution used, almost all masses can be separated, although possible overlapping can still exist. At low mass range, the peak overlapping is neglectable and becomes more possible when increasing the mass range.

Since MBT is a powder, it has been deposited on a substrate to be introduced in the main chamber of the ToF-SIMS. The substrate was, here, a carbon tape, glued on a clean stainless steel block. The mass spectrum was obtained by focusing the primary beam on the powder.

Possible signals coming from the carbon tape cannot be excluded. Nevertheless, the SIMS peak assignment of the MBT powder have been compared to literature data [5] and databases (https://webbook.nist.gov/cgi/cbook.cgi?ID=C149304&Mask=200), making the assignments reliable.

Computational Details

All calculations were performed by applying the framework of DFT with the periodic plane-wave basis set implemented in Vienna Ab initio Simulation Package (VASP) [30,31]. All results reported have been obtained with projector-augmented-wave potentials using a 450 eV plane-wave cut-off [32]. Electron exchange and correlation terms were treated within the Generalized Gradient Approximation (GGA) [33,34]. We used a Methfessel Paxton smearing [35]. Because of the large unit cell size used in calculations, the Brillouin-zone sampling was restricted to the Γ-point. Van der Waals contributions were considered in an explicitly nonlocal correlation term proposed by Dion et al [36] and Klimes et al [37–39] and calculations were carried out using OptB86b-vdw level. More details can be found in [23,40]. Atomic positions were relaxed with the conjugate gradient (CG) algorithm until forces on each moving atom were less than 0.02 eVA^{-1}. The model of the Cu(111) surface with a Cu_2O layer was described in a previous publication [40].

ICP –OES

Immersion corrosion tests were performed at room temperature, in a 0.05 mol/L sodium chloride solution. 1.0 cm² mirror polished copper samples were immersed in 20.0 mL solution. Total immersion time was 21 days. 4.0 mL samplings were taken after 1, 2, 3, 7, 14 and 21 immersion days. After each sampling, fresh corrosive solution was added. This dilution was considered to determine final copper concentration.

To determine copper concentration in solution, an inductively coupled plasma optical emission spectrometer (ICP-OES) ICAP 6300 DUO (Thermo Scientific) was used (ICu = 224.7 nm).

8 standard solutions from 50 ppb to 15 ppm were used. Each solution (volume = 10.0 mL) was acidified with 125 mL 60% (V%V) nitric acid solution. Calibration was validated by a correlation coefficient R^2 superior to 0.999.

The concentration of Cu dissolved is measured. Making the hypothesis that the attack is homogeneous, the thickness loss is equal to $\frac{c \times V}{D \times S}$,

Where *c* is the concentration of dissolved copper measured by ICP, V the volume of immersion, D the copper density, S the sample area. The surface was considered as planar and smooth.

Results

I. XPS and ToF-SIMS analysis of MBT powder

The MBT powder was analyzed using XPS and ToF-SIMS. XPS spectra are in agreement with literature data with one N 1s signal at 400.6 eV, two S 2p signals at 162.4 and 164.6 eV for exo- and endo- cyclic sulfur, respectively. The C 1s signal is at 285.0 eV, typical of C-C bonds. The atomic ratios of the different species are in agreement with the molecule composition (see SI-II section).

These values agree well with those found by Finšgar et *al* [12], who measured for MBT powder a S 2p 3/2 peak for endocyclic S at 164.3 eV, and S 2p 3/2 of exocyclic S at 162.1 eV and with those measured by Wu *et al*. for MBT multilayers on Cu(111), i.e. 164.1 eV for the endocyclic and 162.5 eV for the exocyclic S atoms, respectively. [17]

The MBT molecules were also analyzed by ToF-SIMS. The objective was to define the MBT characteristic mass peaks to be used as references during the analysis of surfaces after exposition to the solution containing MBT. The peaks attributed to the molecules were identified and are presented in **Figure 2** and Table 1 where the measured masses are reported. Note that no peak is observed at the mass corresponding to twice the mass of the molecule, which would reflect the formation of a disulfide bridge between two molecules. However, the absence of a peak does not mean the absence of such a configuration but that if it exists, the radiation of the Bi^+ gun, even if not very intense, is enough to fragment it. Two major peaks are identified at high mass range that are fingerprints of the MBT molecule: a peak at 166.96 amu and one at 165.96 amu, associated to $C_7H_5NS_2^-$ and $C_7H_4NS_2^-$ fragments, respectively. Other peaks are also observed at low mass range, i.e. C_2N^- (38 amu), $^{34}S^-$ (33,96 amu), $^{34}SH^-$ (34,96 amu) and CS^- (43,96 amu). They are characteristic of small fragments of the molecule that are produced during the sputtering process with Bi^+ ions. Nevertheless, one has to keep in mind that $^{34}S^-$ and $^{34}SH^-$ species can also result from air pollution when the powder is transferred to the spectrometer.

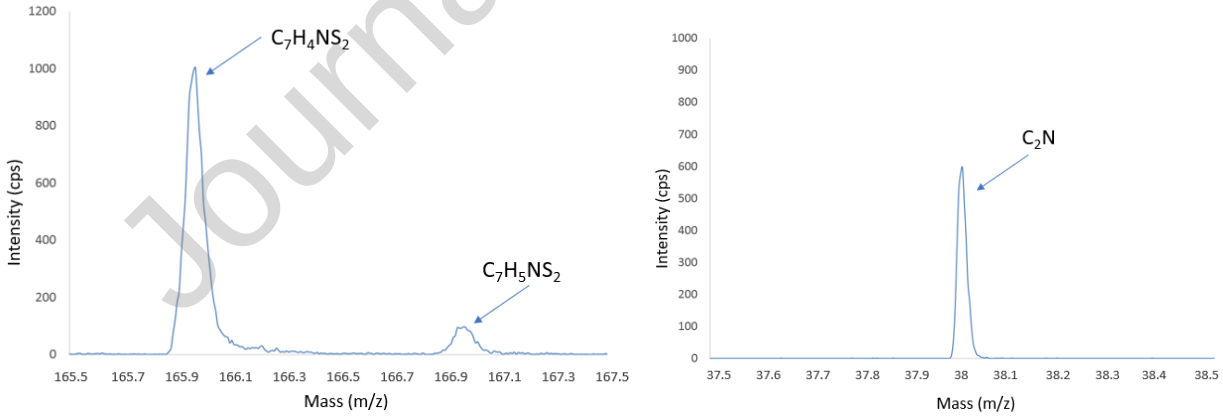

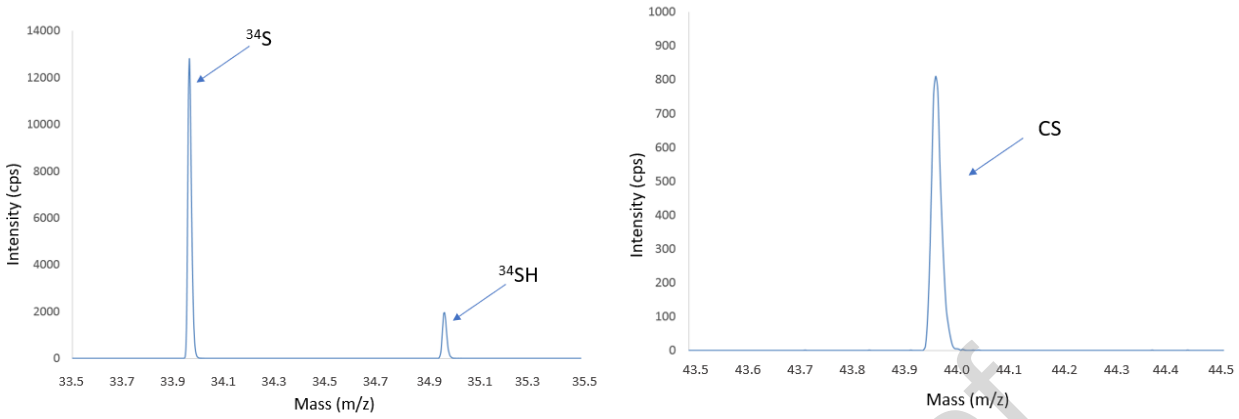

Figure 2 : Mass spectra of the MBT molecule

Table 1: Masses corresponding to the characteristic peaks of MBT powder

Mass (m/z)	Fragment
166.96	$C_7H_5NS_2$
165.96	$C_7H_4NS_2$
38.00	C_2N
33.96	^{34}S
34.96	^{34}SH
43.96	CS

II - Analysis of copper surfaces immersed in MBT solution 1 h and 24 h

II-1-XPS analysis

II-1-1 Survey spectra: chemical elements composing the surface

The general spectra recorded with XPS help identifying the elements present at the surface. An example is shown in **Figure 3**, for copper immersed 1 h in presence of MBT. It shows that the elements present are Cu, C, O, S, and N. No other element is detected. We identify the presence of nitrogen and sulfur which are fingerprints of the MBT molecule. Carbon originates from the molecule but can also be due to carbon contamination. In the following paragraphs, we analyze the high-resolution spectra recorded for each of the components of the surface.

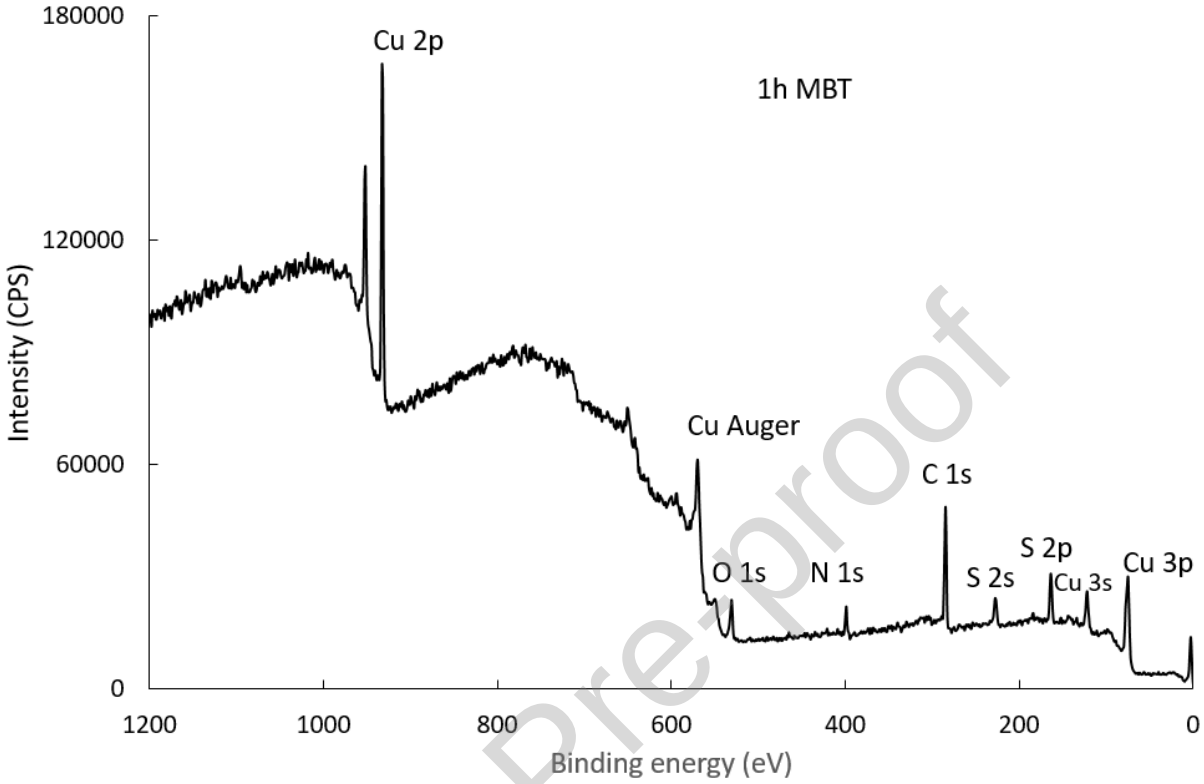

Figure 3 : Survey spectrum recorded for copper immersed 1 h in presence of MBT.

II – 1-2 XPS analysis of S 2p core levels

Figure 4 shows the sulfur S 2p high-resolution spectra of the samples immersed 1 h and 24 h in ultra-pure water solution containing 1.0 mmol. L^{-1} MBT, in comparison with the S 2p region of the sample immersed in ultra-pure water alone. It clearly shows that the sulfur adsorbed on the surface is from the MBT molecule. Indeed, no trace of sulfur was observed on the reference sample immersed in water.

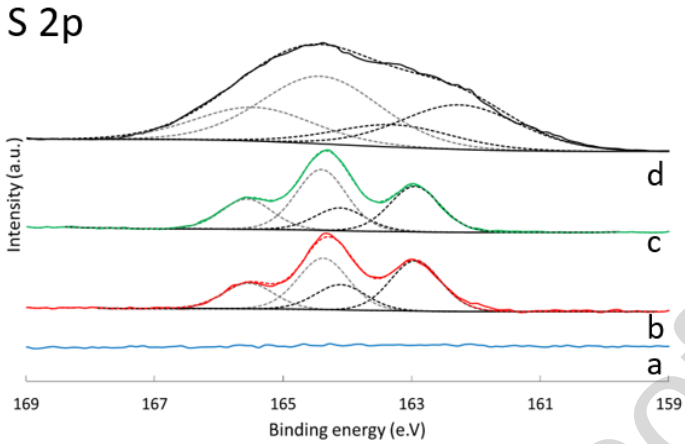

Figure 4: High resolution spectra of the S 2p core level for a-c) copper immersed for a) 1 hour in ultra-pure water, b) 1 hour in 1.0 mmol.L^{-1} MBT solution, c) 24 h in 1.0 mmol.L^{-1} MBT, d) MBT molecule in powder form. The two peaks constituting a doublet (S 2p3/2 and S 2p1/2) are separated by 1.2 eV and the area of the lower binding energy peak is twice the area of the one at high binding energy [41].

The N1s and S 2p peaks associated with the MBT powder have a large width at half height compared to the peaks obtained after adsorption on metal surfaces. This large difference is explained by the fact that the powder is not conductive, which leads to poor evacuation of the charges on the surface during XPS analysis. In contrast, when the molecules are adsorbed on the surface, the charges are removed via the metallic surface.

By comparing the binding energies obtained with respect to those of pure MBT powder, we observe a shift to higher binding energies (BE 163.0 eV, i.e. +0.6 eV) after immersion for 1 h as well as 24 h for the thiol sulfur (located at 162.4 eV in MBT powder). This binding energy shift can be explained by a sulfur-copper bond on the surface. We note that various studies have highlighted the affinity of thiol functions with metal copper surfaces [41] [42]. However, the recorded binding energy does not correspond to the binding energy of thiolate adsorbed on an oxide-free metal surface, as reported in literature, which is 161.9 eV [43]. In contrast, it is in good agreement with the observed binding energy of thiolate on oxide copper nanoparticles, reported in an XPS study of methane thiolate adsorption, in which a S 2p binding energy of 162.9 ±0.1 eV was measured [42]. This suggests that the adsorbed exo S is deprotonated, which means that MBT is adsorbed in the thiolate or in the thione form. Note that both the neutral (thiol or thione) and the thiolate conformers coexist in pure water, considering that the MBT pKa is 6.9.[9] Our

results agree with those of Wu *et al* who found a similar binding energy of 162.3 eV for MBI adsorbed on a 3D-Cu_2O oxide of 1.1 nm thickness [44].

Regarding the endocyclic sulfur, a binding energy 164.4 eV was recorded, thus -0.2 eV with respect to the MBT powder reference. Again, this binding energy corresponds well to previous results of MBT adsorption from the gas phase on pre-oxidized copper (164.1 eV) [43].

After 1 h of immersion, we also detected a very small signal at low binding energy, 161.7 eV, which is typical of thiolate on metallic copper [43]. This signal was not found after 24 h immersion.

II – 1- 3 XPS analysis of N 1s core levels

On the samples immersed 1 hour in ultra-pure water, the N1s spectrum exhibits a weak signal at 400 eV attributed to a slight nitrogen contamination of the surface (**Figure 5**). In contrast, a strong N1s signal is present on the sample immersed for 1 h and 24 h in the presence of MBT. The binding energy is 1.1 eV lower than the position of the peak maximum for the molecule in the MBT powder.

The intensities of N, S_{exo} and S_{endo} were also measured, and the intensity ratios confirm that the molecule is present intact on the surface (SI-III section).

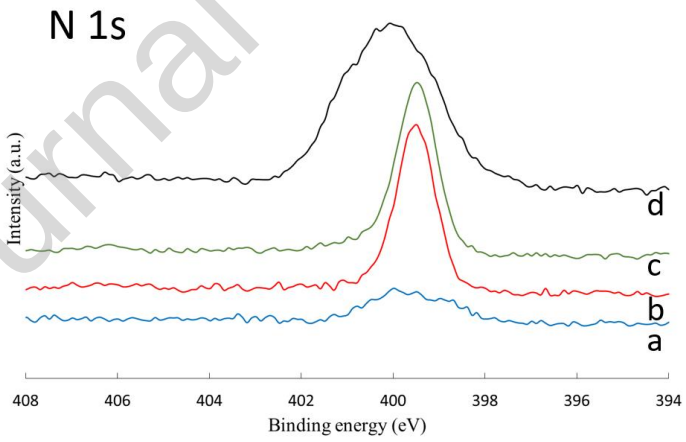

Figure 5: High resolution spectra of the N1s core level for copper immersed for a) 1 hour in ultra-pure water, b) 1 hour in 1.0 mmol.L^{-1} MBT solution, c) 24 h in 1.0 mmol.L^{-1} MBT. d) is for pure MBT in powder form

II – 1- 4 XPS analysis of C 1s core levels: MBT and carbonaceous contamination

It is interesting to analyze the C 1s signal recorded after immersion in presence of MBT. **Figure 6** shows the C 1s regions recorded after 1 h and 24 h immersion with MBT. Three binding energies are identified, at 284.7 ± 0.1 eV (aromatic C-C), 285.5 ± 0.1 eV (C-S and C-N bond) and 286.5 ± 0.1 eV (C=S bond).[43] Note the absence of peaks above 288 eV, that were recorded for Cu immersed in water without MBT (see spectra reported in SI-IV section), which are typical of carbonates and carboxylates, suggesting that MBT inhibits the adsorption of these species.

The spectrum was fitted with components having identical FWHMs of 0.95 eV, very close to the FWHM of 1.0 eV that was used in [17] (**Figure 6**). The area ratios of the peaks are C-S,C-N / $C_{aromatic}$ = 0.47 and 0.53 after 1 h and 24 h of immersion, respectively, and C=S / $C_{aromatic}$ = 0.28 and 0.27 after 1 h and 24 h of immersion, respectively, to be compared with the values of 0.5 and 0.25 in the molecule. We can conclude that the C 1s signal is due in most part to the MBT molecule adsorbed at the surface. Nonetheless, a small amount of adventitious C-C and C-O bonds may be present at the binding energies of 284.8 and 286.4 eV, respectively.[45] An estimation of the possible C 1s contamination may be assessed from the different C 1s ratios. We find that less than 2% of the C 1s signal is due to contamination. The amount of oxygenated contamination can then be assessed: after 1 h and 24 h immersion, we find that 1.6% and 0.9% of C is due to C-O contamination, respectively. This estimation will help us to analyze the O 1s spectrum (see section II-6).

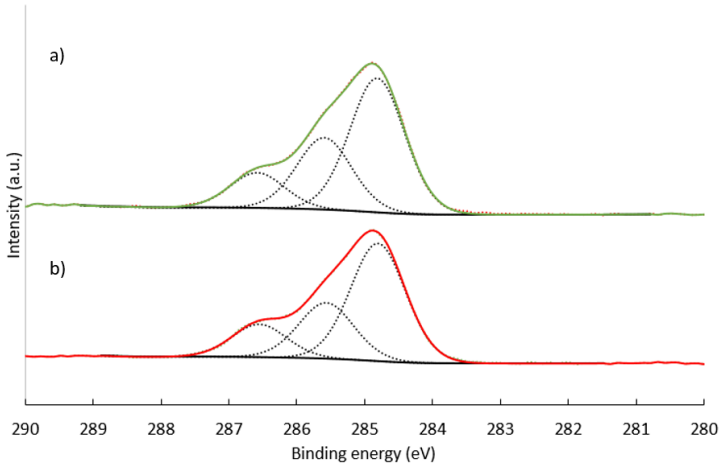

Figure 6 : High resolution spectra of the C 1s core level for copper immersed for a) 24 h in 1.0 mmol.L^{-1} MBT, b) 1 h in 1.0 mmol.L^{-1} MBT solution.

II –1 - 5 Quantitative XPS: surface layers overall composition and thickness

The Cu2p core level spectra (**Figure 7**) show two peaks at binding energies 932.7 eV and 952.4 eV corresponding to $Cu2p_{3/2}$ and $Cu2p_{1/2}$. These binding energies values reflect the metallic state or the Cu (I) state of the cuprous oxide Cu_2O [46–48]. Indeed, the binding energy is the same for these two states of copper and the analysis of the Cu2p spectrum does not allow us to distinguish them. However the analysis of the Auger LMM spectrum can help us to distinguish Cu and Cu_2O [46–48]. Note also the absence of satellite peaks on the spectra, which indicates the absence of Cu(II) for all the samples [46–48]. Thus, the Cu surface is covered with a Cu_2O oxide layer. The thickness of this oxide layer can be calculated, and we obtained using equation (3) (see Experimental details section) a thickness of 3.3 nm on the polished sample, and 6.8 nm after 1 h immersion in water. The attenuation of the peaks after exposure to MBT suggests that the copper surface is covered with an organic layer. In their work, Mansikkamäki *et al* observed a third component in the Cu $2p_{3/2}$ spectra at a binding energy of 934.8 eV that they attributed to Cu (I)-BTA surface complexes [26]. Such a peak is not observed here.

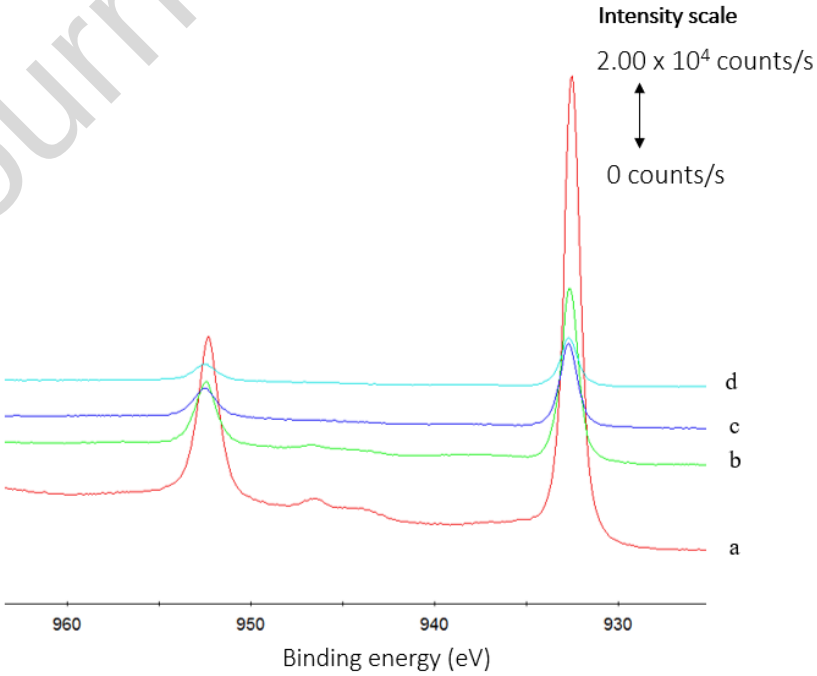

Figure 7: High resolution spectra of the Cu 2p core level for a copper sample a) polished and cleaned, b) immersed for 1 h in ultra-pure water, c) immersed for 1 h in 1.0 mmol.L^{-1} solution, d) immersed for 24 h in 1.0 mmol.L^{-1} MBT solution

The Auger spectra were decomposed with two components obtained from model surfaces produced in the laboratory: one characterizes metallic copper Cu(0), the other cuprous copper Cu(I) (**Figure 8**) [48,49]. The presence of cuprous copper Cu(I) may be related to the formation of copper oxide Cu_2O on the surface, an oxide likely forming during sample preparation and immersion. The O 1s spectrum (**Figure 11**) exhibited a signal at 530.6 eV which is in agreement with the formation of Cu_2O [12]. According to [14], the peak attributed to Cu(I) could also include some contributions from Cu(I)-MBT bonds, typically originating from a MBT layer adsorbed at the oxide surface. The decomposition of the spectra shows that the Cu(0) component associated with metallic copper is clearly less intense on the sample immersed for 1 hour in ultra-pure water without MBT while the quantity of Cu(0) seems similar in the case of copper just polished and copper immersed in the presence of MBT. The Cu(I)/Cu(0) ratio is 3.9 for the polished copper sample and the copper samples immersed in MBT solution, whereas it is 34 for copper sample immersed 1 h in water. This indicates that the growth of the oxide observed in pure water is precluded by the presence of MBT, and that the oxide layer after 1 h immersion has the same thickness as on the polished surface, 3.3 nm. As a final remark, we mention that Cu(I)-MBT complexes have been identified in literature with the Auger peak at 915.3 eV (kinetic energy) [21]. Other authors mention that the Cu-MBT complexes signature is located at 916.5 eV.[14] The present spectra clearly do not exhibit any contribution at 915.3 eV, suggesting that no organometallic complexes are adsorbed on the surface.

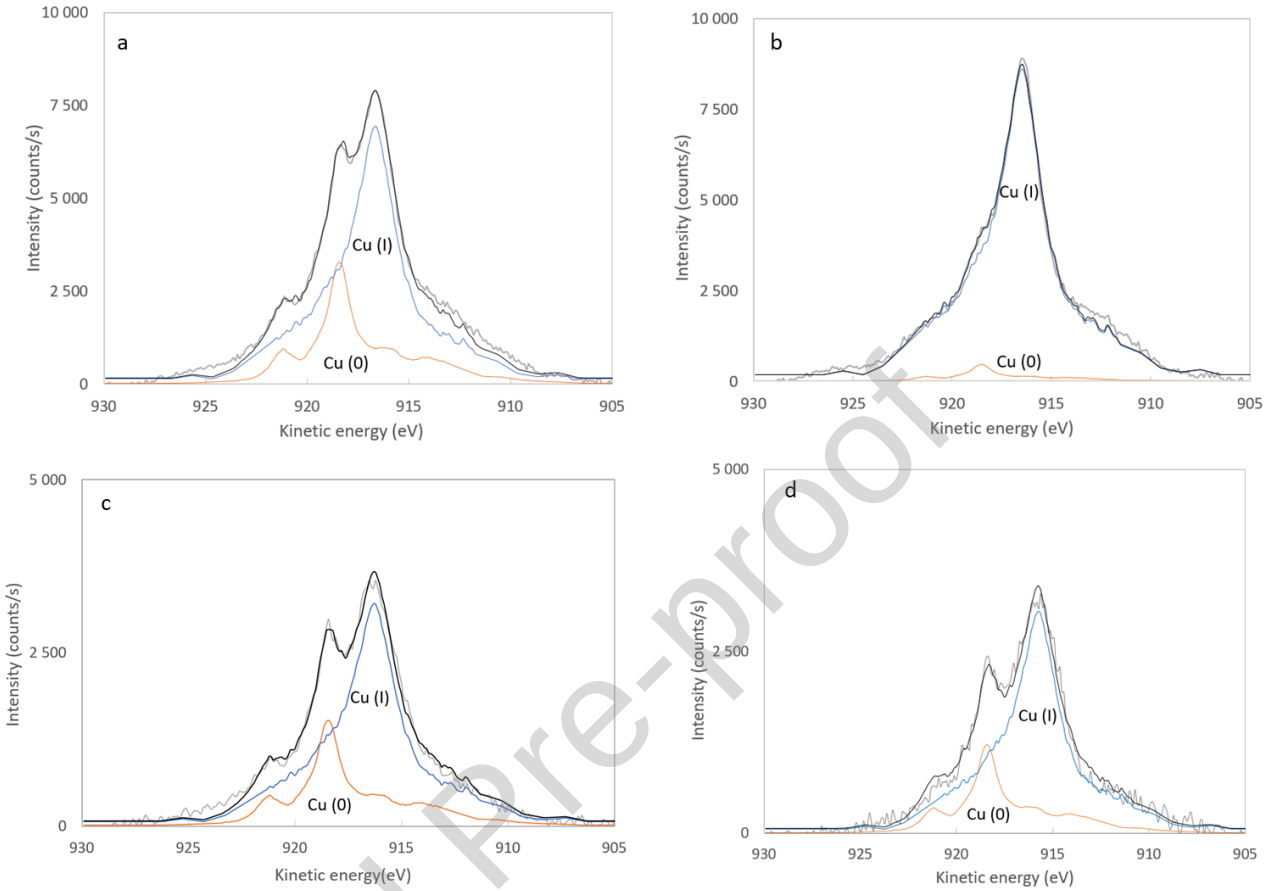

Figure 8: Auger Cu LMM spectra for copper a) polished and cleaned, b) immersed for 1 h in ultra-pure water, c) immersed for 1 h in 1.0 mmol.L^{-1} MBT solution, d) immersed for 24 h in 1.0 mmol.L^{-1} MBT solution

Once the oxide thickness estimated, the thickness of the MBT layers were calculated using equations (4) and (5) (see experimental details section). In this calculation, the density of adsorbed MBT is that of the MBT powder. After 1 hour of immersion, the estimated MBT layer thickness is ~ 2.1 nm, and ~ 3.0 nm after 24 h of immersion. Seen the size of the molecule (0.6 to 1.2 nm, depending on the molecule orientation), these thicknesses correspond to multilayers of MBT. A more sophisticated quantitative treatment taking into account the bilayer nature of the MBT layer will be done below, without significative changes to this result.

II – 2 ToF-SIMS analysis of the MBT-surface binding mode

To further characterize the adsorbed layer and determine the adsorption mode of the molecules, additional analyses were carried out by ToF-SIMS.

A copper sample immersed for 1 h in ultra-pure water and used as a reference (denoted reference substrate in the following) and a sample immersed for one hour in an ultra-pure water solution containing 1.0 mmol.L^{-1} of MBT were analysed. The general TOF spectra are reported in SI-V section.

The analysis of the peaks of the characteristic fragments of MBT in the high mass range (**Figure 9**) shows that the molecule is indeed present on the copper surface immersed for 1 hour. The intensity (normalized units) of the peak at 166.96 amu, associated to $C_7H_5NS_2^-$, is $9.4x10^{-3}$ ($8.2x10^{-4}$ for the reference sample), and the intensity of the peak at 165.96 amu, associated to $C_7H_4NS_2^-$, is $9.2x10^{-2}$ ($5.3x10^{-3}$ for the reference sample). A trace amount signal is observed on the reference copper surface. A slight contamination may have occurred during sample preparation and transfer into the UHV analysis chamber of the ToF-SIMS spectrometer (the reference sample and the sample exposed to MBT were introduced together in the spectrometer) or during the analysis.

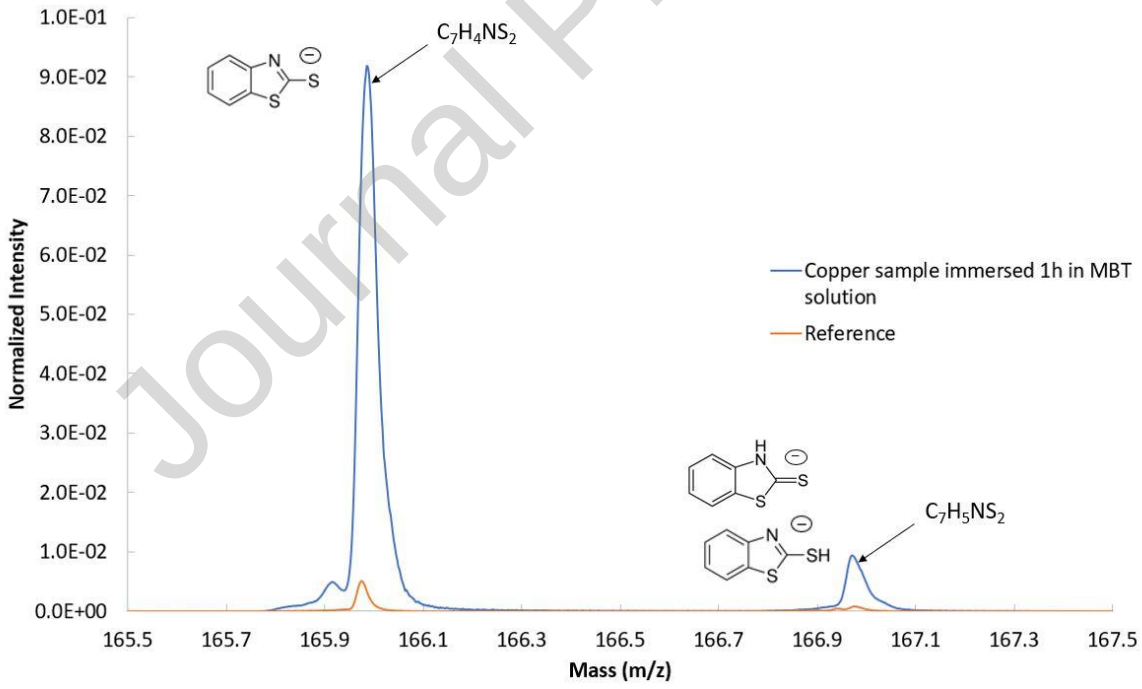

Figure 9: Mass spectra characteristic of MBT on the copper surface after immersion in aqueous solution with MBT for 1 hour, and spectra obtained for the reference copper sample (not exposed to MBT). Intensity values are relative to the total intensity of the secondary ions, which is arbitrary normalized to 100 in order to compare both spectra.

In-depth profiles were then recorded and are presented in **Figure 10**. We note that the intensity of the fragment corresponding to MBT minus one H ($C_7H_4NS_2^-$) exhibits a high intensity on the surface, and drops immediately when probing the subsurface region. Considering the soft sputtering conditions used to get the in-depth profiles, this finding indicates that the surface layer of organic MBT molecules is ultra-thin.

Profiles of lighter fragments were recorded to investigate the orientation of the molecule on the surface. By following the C_2S^-, $^{34}S^-$ and C_2N^- characteristic fragments of the MBT molecule (based on analysis of the MBT powder, see **Figure 2**), one observes that these fragments reach their maximum intensities for longer sputtering times than the maximum intensity of the $C_7H_4NS_2^-$. Thus, although $C_7H_4NS_2^-$ and all the small fragments (C_2S^-, $^{34}S^-$ and C_2N^-) are characteristic species of the MBT molecule (see **Figure 2**), the identification of the smaller fragments (C_2S^-, $^{34}S^-$ and C_2N^-) closer to the substrate than $C_7H_4NS_2^-$ indicates that different configurations of the adsorbed MBT molecules coexist. The presence of a strongly bonded MBT monolayer on the Cu surface would explain the presence of smaller S and N containing fragments (C_2S^-, $^{34}S^-$ and C_2N^-) whereas the intensity of the $C_7H_4NS_2^-$ fragment is low. On the contrary, the $C_7H_4NS_2^-$ fragment observed in the outer part would be associated to the formation of a weakly bonded layer, probably a multilayer as observed by XPS, easily and immediately removed during the first ToF-SIMS sputtering cycles.

Looking deeper at the strongly bonded inner monolayer which covers the Cu substrate, one can observe that the fragments containing the sulfur atoms (C_2S^-, $^{34}S^-$) reach their maximum intensity after the fragment containing the nitrogen atom (C_2N^-) thus indicating that the sulfur atoms are located deeper than the nitrogen atoms. In addition, the intensity of the sulfur-containing fragments starts to drop when the intensity of the $^{65}CuO^-$ fragments (characteristic of the Cu oxide layer) reach its maximum intensity. This observation indicates that the majority of MBT molecules are bonded to the oxidized copper surface via the sulfur atoms. We have however observed the presence of a peak at the mass corresponding to the fragment Cu_2SNC^-, i.e. a fragment of the molecule associated with copper atoms (Cu_2SNC^-). This may indicate either that the molecule on the oxide is desorbed with the Cu atoms (and not a Cu-O fragment), and/or that a possible and local adsorption of MBT on metallic Cu exists via Cu-S bond. The latter adsorption mode is confirmed by XPS with the presence of a small peak at 161.9 eV, typical of the S-Cu metal bond. Considering the sensitivity of ToF-SIMS compared to XPS, it is not surprising to detect, with ToF-SIMS, species that represent only a fraction of the overall MBT amount.

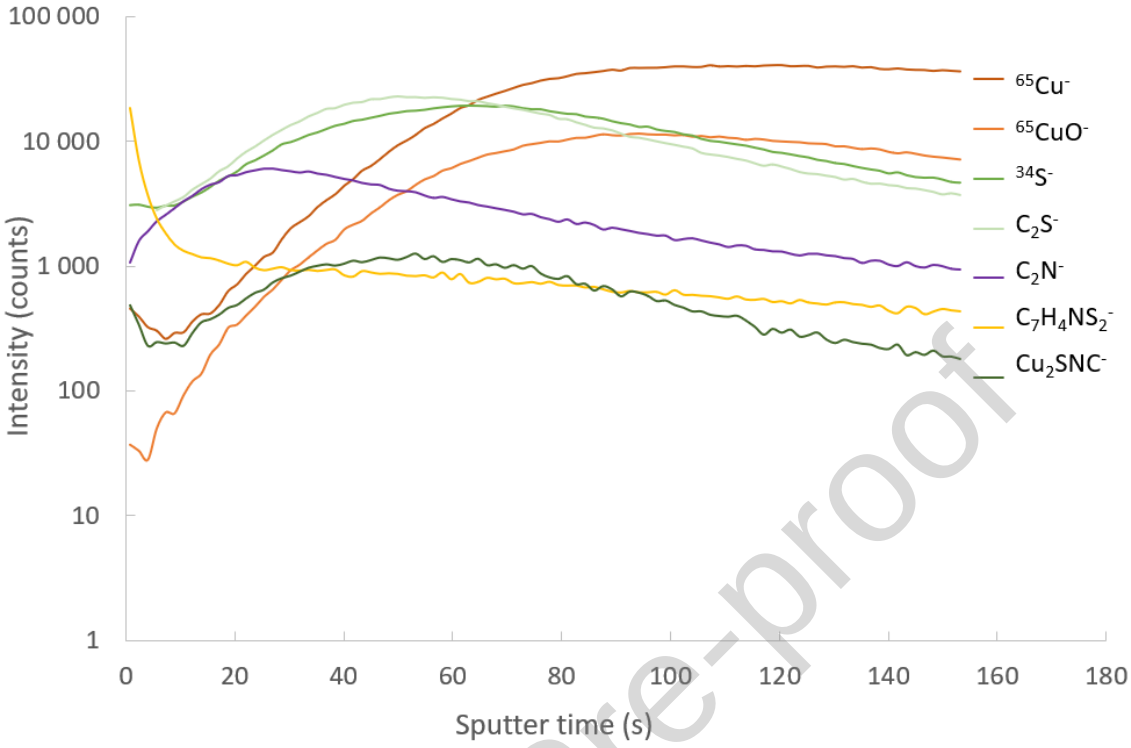

Figure 10: In-depth profiles measured by ToF-SIMS for the copper sample immersed for 1 hour in aqueous solution with MBT

The combined use of XPS and TOF SIMS allows us to propose a stratified model of the outermost surface layers: the copper surface is oxidized in Cu_2O, and the oxide layer (thickness 3.3 nm) is covered with one of several MBT layers. The MBT layer consists in an inner monolayer of MBT molecules adsorbed on the Cu oxide surface, with a small fraction of molecules bonded to metallic copper, and covered by weakly bonded (physisorbed) MBT molecules.

II – 6 Identification of co-adsorbed water

Figure 11 shows the XPS O 1s spectra recorded for copper immersed in water with MBT for 1 h and 24 h. The O 1s spectrum exhibits two components. The first one at 530.5 eV is attributed to O^{2-} in copper oxide. This signal is smaller after 24 h immersion in presence of MBT as compared to 1 h immersion. This is due to signal attenuation by a thicker adsorbed MBT layer after 24 h immersion. The second peak, named for convenience O_{high}, is located at 532.7 eV, and has the same intensity after 1 h and 24 h immersion, suggesting that this species is not attenuated by the organic layer, but rather located either at the same place or above. This peak can be attributed either to oxygen bound to adventitious carbon, named O_C, or to water (O_{H2O}) at the surface. We have shown in section II-1-4 that 1.6% and 0.9% of total C is adventious

carbon bound to one O, so Oc is known. Subtracting this O_C contribution from the O_{high} peak, we find a ratio of O of 5.5% of the total (carbon+ O_{high}) amount (1 h immersion) and 4.9% of the total (carbon+ O_{high}) amount (24 h immersion) which is due to O_{H2O}. It corresponds to a ratio of water/MBT of 29% after 1 h adsorption and 27% after 24 h adsorption. This result suggests that some water molecules are strongly bound to the MBT layer and are not desorbed in UHV. This finding is further confirmed by the presence of small peaks of HO_2^- and OH^- species, identified with ToF SIMS in the depth profile (not shown).

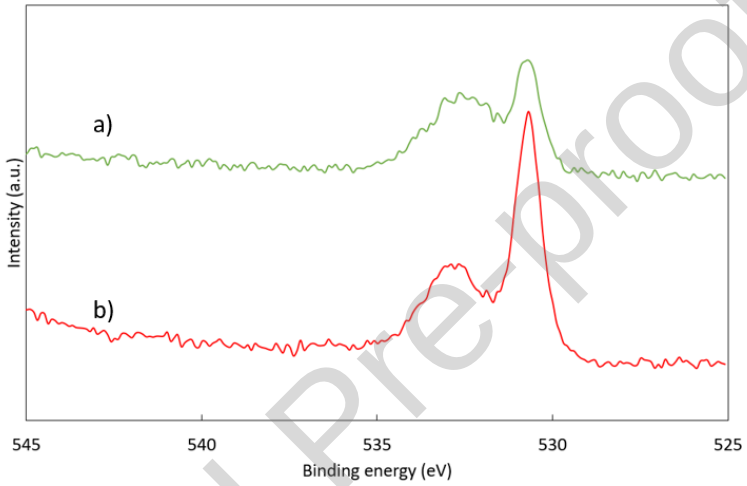

Figure 11 : High resolution O 1s core level spectra for a copper sample immersed for a) 24 h (green) and b) 1 h (red) in 1.0 mmol.L^{-1} MBT

III- Immersion in presence of chlorides

The samples were also immersed in NaCl and NaCl + MBT, for 1 h. The Cu, S and N spectra recorded were very similar to those in pure water and pure water + MBT, respectively. They are reported in the SI-VI section. We just mention here that the presence of chloride does not modify the MBT layer formation, as the S/Cu ratio is identical to that after immersion in pure water. Also, the Cu(I)/Cu ratio is of the same order as in pure water (see SI-VI section), indicating that as in pure water, MBT inhibits the oxide growth. More attention has been paid to the Cl 2p signal. We mention that no Na 1s signal was recorded, indicating that Cl was present in the form of chloride in the oxide film. The binding energy (200.0 eV) is associated to chlorides

([27,50,51]). **Figure 12** presents the Cl 2p spectra recorded after immersion 1 h in pure NaCl, 1 h in NaCl + MBT, and 24 h in NaCl + MBT. We clearly notice that the amount of Cl is inferior in presence of MBT than in NaCl after 1 h, and that after 24 h no more Cl is present at the copper surface. The quantitative analysis shows that the Cl amount falls from 2.9% at. in absence of MBT to 0.5% at in presence of MBT.

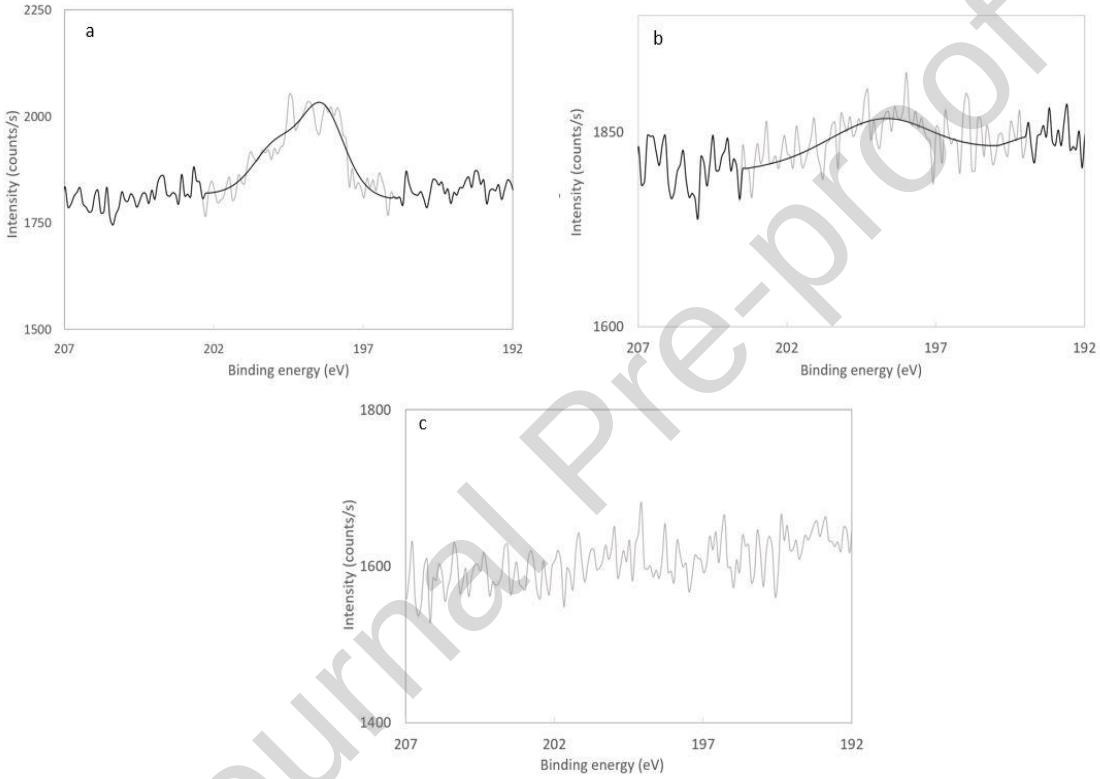

Figure 12 : Cl 2p spectra recorded after a) 1 h in NaCl solution, b) 1 h in NaCl + MBT solution, c) 24 h in NaCl + MBT solution

IV- Corrosion resistance : ICP OES experiments

The ICP measurements were performed after several immersion times (in days) in NaCl and NaCl + MBT solutions. Results were repeated three times and averaged (**Figure 13**). The effect of MBT is very clear: whereas Cu dissolution is high in NaCl, it is very attenuated when MBT is adsorbed on the Cu surface.

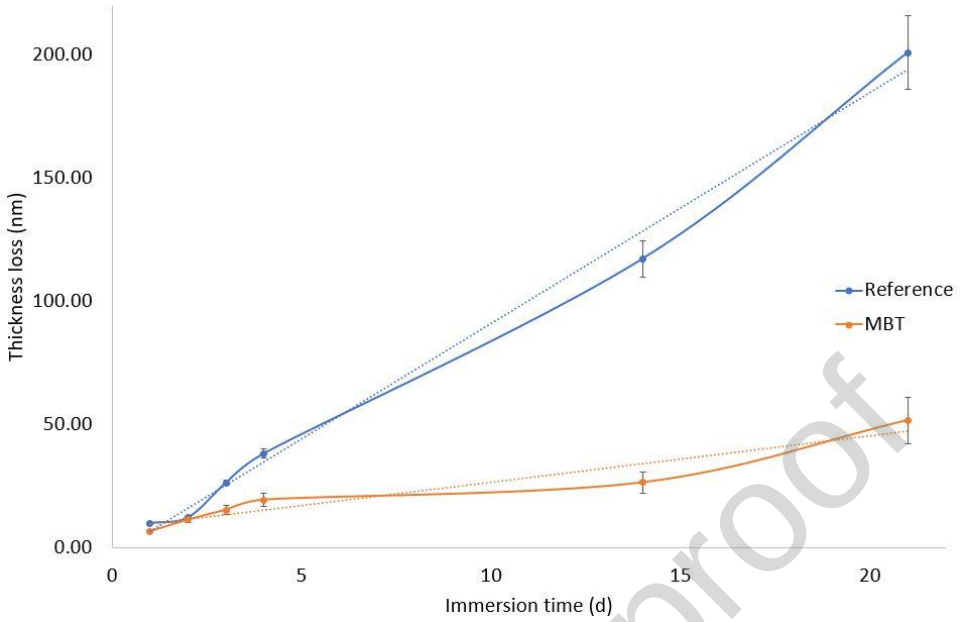

Figure 13: Thickness of Cu dissolved with time determined by ICP-OES measurements on Cu immersed in NaCl (blue curve) and NaCl + MBT (orange curve) solutions.

III - Discussion

III-I- A model of Cu covered with MBT

The XPS data show that the MBT molecule is adsorbed on copper oxide, with binding energies of 399.5 eV for N 1s, 164.4 and 163 eV for S endo and exo-cyclic, respectively. The amount of adsorbed MBT increases from 23 to 32 Å from 1 h to 24 h immersion of copper in the aqueous solution with MBT. The mass spectra recorded by ToF-SIMS also show the presence of molecules adsorbed on the surface. In the early sputtering stage, the physisorbed molecules located at the extreme surface may have been removed and only the chemisorbed layer strongly bonded to the surface was analyzed.

Table 2 gives the different S 2p and N 1s binding energies taken from data reported in previous studies of MBT adsorption on Cu. The different XPS results and assignments are now discussed.

For MBT adsorbed on metallic Cu there is a general agreement that the thiolate function is involved in a bond with Cu, and the resulting S 2p binding energy is 161.6 eV. In their work on a model system, Cu metal exposed to MBT in gas phase, Wu et al [43] recorded only one single S 2p signal at this value and concluded that the molecule is adsorbed through both S atoms, which exhibit the same binding energy. As

for the N 1s peak, it was measured at 389.8 eV. To the best of our knowledge, no interpretation has been proposed for this binding energy, which can be due to deprotonation of the NH function or/and chemical bond with copper. DFT calculations have confirmed that the bonding of MBT with the oxide-free metal surface occurs via the exo- and endo-cyclic sulfur atoms [52]. In the present work, such a S 2p signal at 161.7 eV is observed with a weak, but significant, XPS intensity.

On a pre-oxidized Cu sample, Wu et al [43] have shown that the MBT adsorbs in substitution to oxygen, giving rise to the same binding energies of S and N, confirming that MBT displaces the 2D-oxide and binds to the underlying metal. At higher coverage, signals at 162.5, 164.1 eV for S and 399.0 eV for N 1s appear. This can be due either to molecules in a multilayer, or molecules adsorbed on the oxide surface. Indeed, on 3D oxide, peaks at 162.5, 164.1 eV for sulfur and 399.4 for nitrogen were observed. Our measurements for adsorption from the liquid phase are in agreement with these results and allow us to confirm that the binding energies recorded for the main S 2p peaks and the N 1s peak are characteristics of the adsorption of MBT on Cu oxide. These binding energies are also in agreement with those measured by other authors [17] [32] (see Table 2). It is interesting to note that the recorded S 2p binding energies differ from those of Kazansky *et al* [21] and Arkhipushkin *et al* [53], 163.5 and 165.1 eV, attributed to adsorbed Cu-complexes. Moreover, the Cu Auger spectra do not exhibit low kinetic energy signal at 915.3 eV that have been attributed to Cu-complexes.[21] Even if the Cu(I) KLL contribution could contain some Cu(I)-MBT contribution [14], the absence of MBT-Cu complex signature in the S and N spectra suggests that complexes, if present, would not be in significant amount.

Table 2: Review of XPS data for the S_{exo}, S_{endo} and N atoms for the MBT- Cu system in different environments

Exposure conditions	Powder	Gas phase			Neutral water phosphate solution (pH 7.4)	Neutral borate buffer solution with 0.5 M NaCl (pH 7.4)	5 mM H_2SO_4 solution (10 min)	Aqueous 3wt.% NaCl solution.	Cu-MBT precipitation	0.5 M NaCl solution under N_2 (pH 3)	Aqueous solution 1 h	Aqueous solution 24 h
Surface State	/	Metallic Cu	Pre oxidized Cu	Oxidized Cu	Oxidized Cu	Oxidized Cu	Oxidized Cu	Oxidized Cu	Tridimensional compound Cu-MBT	Metallic Cu	Oxidized Cu	Oxidized Cu
C 1s position (eV)	285.0	284.8	284.8	284.8	285.0	285.0	285.0	284.8	285.0	285.0	285.0	285.0
S $2p_{3/2}$: exo sulfur (S2) (eV)	162.4	161.4: on metal 162.5: multilayer	161.6 at low coverage, 162.5	162.5	163.4: complex formation	~163.2 : complex formation	162.8	162.1	162.9	One peak id. powder (164.1)	163.0	163.0
S $2p_{3/2}$: endo sulfur (S1) (eV)	164.6	161.4: on metal 164.1 eV: multilayer	161.6 at low coverage, 164.1	164.1	164.8	~165.1	164.2	164.3	164.4		164.4	164.4
N 1s (eV)	400.6	399.8: on metal 399.1: multi layer	399.8 at low coverage 399.0	399.4 (multi layer)	399.5: complex formation	399.9 : complex formation	399.5	398.8		400.1	399.5	399.5
Attribution / Interpretation	/	Adsorption through both S atoms + multilayer formation	Adsorption through both S atoms	Adsorption through both S atoms + multilayer formation	Complexes multilayer (through Sexo and N atoms)	Polymeric film Cu (MBT) complexes (through Sexo and N atoms)	Chemisorbed monolayer mainly through the Sexo atom	Adsorption through the Sexo and N atoms			Adsorption through Sexo and S endo	
Organic layer thickness	/	Monolayer: 0.2 nm		Monolayer: 0.2 nm	Depending on exposure	Depending on exposure	1.0 nm	1.5 nm		MBT-Cu	2.3 nm	3.2 nm

		Multilayer: 0.6 nm		Multilayer: 1.0 nm	time (up to 8-9 nm)	time (up to 6-7 nm)				complex		
Reference	This work	Wu *et al* (2020) [17]			Kazansky *et al* (2012) [21]	Arkhipushkin *et al* (2014) [22]	Tan *et al* (2004) [54]	Finšgar *et al* (2014) [12]	Goh *et al* (2008) [55]	Chadwick *et al* (1979) [14]	This work	This work

The review of XPS data for MBT on Cu (Table 2) shows that only the binding energy of S on metallic copper is unambiguously assigned, with a low S 2p binding energy (161.9 eV), allowing us to conclude that after 1 h of immersion, a fraction of MBT is adsorbed on non-oxidized patches of the otherwise totally oxidized copper surface.

The detection by ToF-SIMS of MBT-Cu species (Cu_2SNC^-) can be assigned to i) MBT adsorbed on metallic copper, ii) MBT adsorbed on Cu_2O, ejected with two Cu atoms, iii) Cu-MBT complexes. We now examine the three hypotheses:

i) On Cu metal, model experiments [43] and previous DFT calculations [52,56,57] have established the adsorption through the S atoms, forming strong bonds with Cu. In addition, previous DFT calculations have shown that MBT can heal depassivated surfaces in adsorbing on metal areas [56]. The identification of the Cu_2SNC^- is in agreement with these findings.

ii) On Cu_2O, according to previous DFT calculations, MBT thione adsorbs on top of an unsaturated Cu, forming a Sexo-Cu bond. In the S S orientation to the surface, only one S does a bond with a Cu surface atom, as shown in **Figure 14** hereunder. This cannot explain the identification of (Cu_2SNC^-) species, where two Cu are ejected. In the thiolate form, an additional N-Cu bond is formed with a saturated surface Cu. However, this possibility disagrees with the observed orientation of MBT, with the two S directed towards the surface.

iii) Finally, the possibility of the presence of some Cu(I) MBT complexes within the organic layer cannot be excluded, but their amount would be very low as it is not detected by XPS in this work.

Finally, the identification of MBT-Cu fragments, together with a XPS signature of MBT on the metal, and the full agreement with DFT calculations lead us to conclude in favor of MBT adsorbed at metallic Cu on a small fraction of the surface. This could be due either to the healing by MBT of uncovered metallic zones (which can explain that MBT is a barrier against Cu oxidation), or to the reduction of Cu_2O by MBT at some places, as already proposed in the literature. [17]

On oxidized Cu and in MBT multilayers (on metal or oxide), the binding energies are 164.4, 163.0 eV for S 2p and 399.5 eV (multilayer on metal) and 399.4 eV (monolayer and multilayer on oxide) for N 1s. Whereas it is admitted that the exo S is deprotonated when adsorbed, a result also obtained in recent DFT calculations ([23,56]), the exact binding mode of MBT (through one, two S or through the exo S and the N atoms) to the oxidized Cu surface cannot be totally disentangled with XPS. The ToF-SIMS profiles made

it possible to determine that the atoms closest to the surface are the sulfur atoms. Water being co-adsorbed with MBT, the N(H) group might be in H bond interaction with OH groups or co-adsorbed water molecules.

In recent works [23,56] we showed using DFT calculations that the MBT molecule can adsorb on a pre-oxidized Cu surface via the exo S and the NH group for the thione form and via S and N atoms for thiolate species [23]. According to these previous calculations, the –S –N configuration is more stable than the –S –S configuration by 0.17 eV and 0.36 eV for the thiolate and thione conformer, respectively. This result seems to be in disagreement with the present work, where we identify rather an orientation of the molecule with both S oriented towards the surface. To understand this apparent discrepancy, we performed additional DFT calculations. As XPS analysis has revealed the presence of co-adsorbed water with MBT, we modelled a full layer of MBT adsorbed on pre-oxidized copper, both in the –S–S and the –S–N orientations, with co-adsorbed water, as shown in **Figure 14**. The thione conformer was chosen because of the highest energy difference between –S –S and –S –N configurations, as it is favorable by 0.36 eV to the –S –N configuration. As already described in our previous works, the adsorbed MBT molecules are bonded to the surface through one S-Cu bond with an unsaturated Cu. In the –S –N orientation, an additional H bond between NH and a O surface atom is formed.[23] More details of these configurations are given in ref [23]. The MBT monolayer density is 3.27 molecule/nm^2. Note that this density is lower than that calculated for standalone SAMs of MBT (4 to 4.6 molecule/nm^2),[52] so it is possible to insert water molecules in it. To do this, we added one, two and three water layers (one water layer corresponds to one water molecule per unsaturated Cu surface atom). The first water layer adsorbs by making H bond with unsaturated surface oxygen atoms. The adsorption energy per water molecule is -0.66 eV for the –S –S configuration and -0.32 eV for the –S –N configuration. This difference is due to the fact that in the –S –S configuration, the unsaturated oxygen surface sites remain free (non bound) without the presence of water in the MBT organic layer and thus are available to accept a H-bond from water. In contrast, in the –S –N configuration, water competes with the NH group in forming a H bond with the surface, thus the contribution of water co-adsorption at the interface is lower in the -S -N configuration than in -S –S one, with an energy difference of 0.34 eV per water molecule. As the –S –N configuration was more stable by 0.36 eV than the –S –S one, with water the two orientations are iso-energetic.

Adding a second water layer is exothermic, with adsorption energies of -0.68 eV and -0.34 eV for the –S –S and –S –N structures, respectively. This time, in the –S –S configuration, water makes a H bond with the NH group, and this brings an additional stabilization. In contrast, no H bond is formed between water and $–S_{endo}$ group of the –S –N configuration, thus adsorption of the second water layer is also exothermic, but less favored. Now, the –S –S configuration is more stable by 0.31 eV per molecule than the –S –N configuration.

Adsorption of the third water layer is exothermic in both configurations, -0.37 and -0.39 eV/molecule for –S –S and –S –N, respectively. Water adsorbs now without any specific interaction with the MBT molecule, making an H bond with the underneath water layer. The prevalence of the –S –S configuration over the –S –N one is not modified.

All in all, for the –S –S configuration, a strong stabilization occurs with the formation of H_2O—surface (first water layer) and H_2O—NH (second water layer) bonds. In contrast, for the –S –N configuration, there is no specific stabilizing effect of water adsorption, which adsorption energy is not layer-dependent, all energies being typical of water adsorption with H bonds formation and water-water interaction in water multilayer on solids.[58,59]

A last remark must be done on the amount of water introduced in the MBT layer in the DFT calculations, which is much higher (2 to 3 water molecules per MBT molecule) than the experimentally measured value of 28% H_2O/MBT. We think that desorption of a part of the water co-adsorbed with MBT in the UHV apparatus cannot be excluded.

DFT is also useful to specify the in-depth densities of the adsorbed layers. According to our calculations, the density of the first MBT layer is 3.27 molecule/nm^2 and its thickness is 7 Å. These numbers were injected in the layer-by-layer model of adsorbed MBT (see equation (5')), and we found, considering that the MBT density in the multilayer is that of MBT in powder, a thickness of 16 and 25 Å of physisorbed MBT above the chemisorbed MBT layer after 1h and 24h immersion, respectively. This gives a total thickness of 23 and 32 Å respectively, for 1 and 24 h immersion.

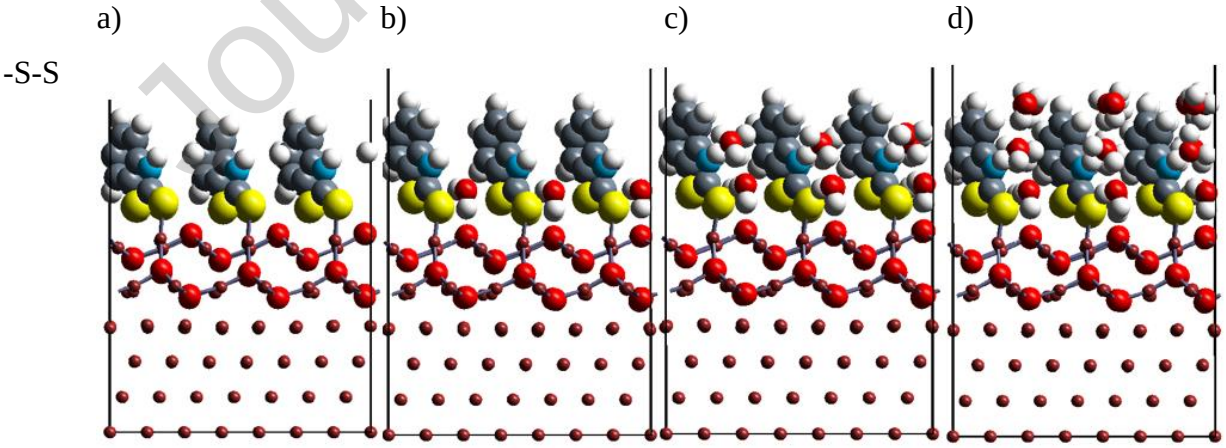

-S-N

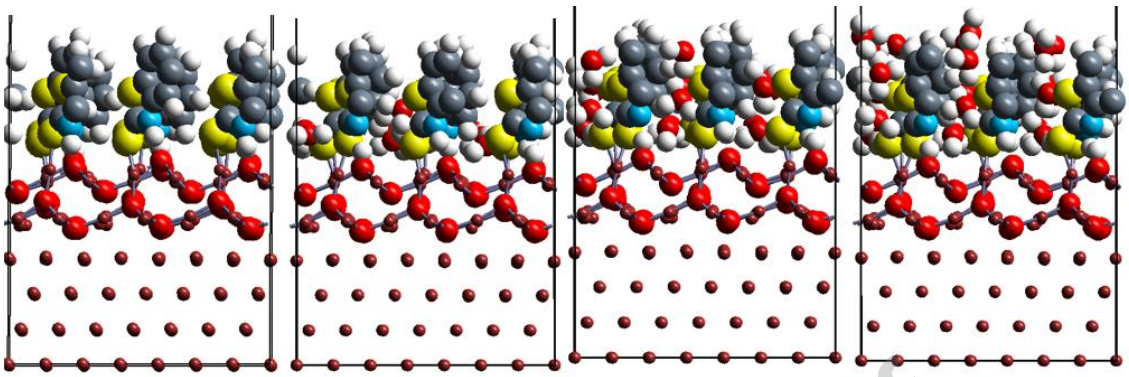

Figure 14: Configurations of MBT adsorbed on a Cu_2O layer on Cu, (a) without and with (b) one, (c) two and (d) three co-adsorbed water layers. Upper panel: -S–S orientation, lower panel : -S-N orientation. Color code: small red, Cu; big red, O; yellow: S; black: C; white: H ; blue: N atoms.

III-2 Inhibition properties

The corrosion inhibition properties of the surface covered with MBT have been demonstrated with ICP-OES. In addition, XPS measurements have evidenced that MBT is adsorbed on the Cu surface in the same amount without and with Cl^-, and inhibits the oxide growth. Both facts, together with DFT calculations which show the formation of MBT-Cu bonds, and the identification of MBT-Cu ions with ToF-SIMS, suggest that MBT blocks the surface Cu atoms, which are then unavailable for adsorption of water, OH or Cl^-. Interestingly, MBT does not inhibit water entry which is co-adsorbed with MBT, but no Cu surface site is further available for OH adsorption and further oxide growth. Moreover, we have evidenced the presence of MBT adsorbed at metallic zones. Those zones are likely the places of favored dissolution, where oxidation may take place. The fact that MBT is adsorbed at these metal zones certainly blocks both oxidation and dissolution.

Finally, MBT inhibits the entry of Cl in the oxide layer. The results suggest that MBT/Cl adsorption competition is in favor of MBT. This result confirms previous DFT calculations. Indeed, Gustincic and Kokalj calculated a binding energy of 3.00 eV for Cl on copper oxide surface [60]. This value is smaller than that reported for thione adsorption on the same surface, 3.4 and 3.1 eV at low and high coverage, respectively [61].

It appears thus clearly that MBT and Cl adsorption are competitive, and in favor to MBT, and that the inhibition of Cl ingress at the surface and in the oxide film results in corrosion protection. It may be also

possible that as Cl, OH penetration and diffusion in the oxide film is prevented by MBT, thus the oxide growth mechanism by anion diffusion is inhibited.

IV - CONCLUSIONS

The combination of XPS and ToF-SIMS analyses, and the complementary DFT calculations, have allowed us to better characterize and understand the adsorption of MBT on Cu surfaces in water. The main conclusions are the following:

i) MBT is adsorbed on the oxide and forms multilayers with thicknesses of 2.3 to 3.2 nm after immersion of copper samples in aqueous solution containing MBT for 1 h to 24 h immersion, respectively; this layer is composed of an inner chemisorbed MBT layer of thickness 7 Å, and an outer physisorbed multilayer. The carbonaceous contamination on the surface is less than 2% atomic.

ii) MBT adsorption also occurs after immersion in NaCl + MBT, in the same amount as in pure water,

iii) Adsorbed MBT inhibits the copper oxide growth, in water and NaCl solution,

iv) The first MBT layer close to the substrate is more strongly bonded than the outer MBT layers, has a thickness of 7 Å and a density of 3.27 molecule/nm^2. The MBT bonding to copper is via the two S atoms oriented towards the copper oxide surface,

v) Co-adsorbed water is trapped in the MBT layer (the ratio H_2O/MBT is 0.28), and likely interact via H bonds with the N(H) group, as suggested by DFT calculations,

vi) A fraction of MBT is (covalently) adsorbed on metallic copper, healing some depassivated areas, as revealed by the ToF-SIMS in-depth profiles and XPS.

vii) MBT adsorption decreases the adsorption of Cl on the Cu surface,

viii) MBT adsorption inhibits Cu dissolution, even after 20 days immersion in NaCl

Thus, we demonstrated that MBT, by adsorbing and forming a full monolayer at the Cu surface, both on the Cu_2O oxide and at metal zones, inhibits further oxide growth and copper dissolution in NaCl.

AKNOWLEDGEMENTS

Région île-de-France is acknowledged for partial funding of the ToF-SIMS equipment. The authors thank SOCOMORE for funding and GENCI for high performance calculations in the national (CINES) center under the agreement A0040802217.

REFERENCES

[1] S. V. Lamaka, M.L. Zheludkevich, K.A. Yasakau, M.F. Montemor, M.G.S. Ferreira, High effective organic corrosion inhibitors for 2024 aluminium alloy, Electrochimica Acta. 52 (2007) 7231–7247.

[2] G. Zhou, Y. Feng, Y. Wu, T. Notoya, T. Ishikawa, Corrosion Inhibition of Copper by 2-Mercaptobenzothiazole and Benzotriazole in Low-Conductivity Solutions, Bull. Chem. Soc. Jpn. 66 (1993) 1813–1816. https://doi.org/10.1246/bcsj.66.1813.

[3] S.B. Sharma, V. Maurice, L.H. Klein, P. Marcus, Local Inhibition by 2-mercaptobenzothiazole of Early Stage Intergranular Corrosion of Copper, J. Electrochem. Soc. 167 (2020). https://doi.org/10.1149/1945-7111/abcc36.

[4] R. Subramanian, V. Lakshminarayanan, Effect of adsorption of some azoles on copper passivation in alkaline medium, Corros. Sci. 44 (2002) 535–554. https://doi.org/10.1016/S0010-938X(01)00085-3.

[5] M. Finšgar, Surface analysis of the 2-mercaptobenzothiazole corrosion inhibitor on 6082 aluminum alloy using ToF-SIMS and XPS, Anal. Methods. 12 (2020) 456–465.

[6] K. Xhanari, M. Finšgar, The Corrosion Inhibition of AA6082 Aluminium Alloy by Certain Azoles in Chloride Solution: Electrochemistry and Surface Analysis, Coatings. 9 (2019) 380. https://doi.org/10.3390/coatings9060380.

[7] A.C. Balaskas, M. Curioni, G.E. Thompson, Effectiveness of 2-mercaptobenzothiazole, 8-hydroxyquinoline and benzotriazole as corrosion inhibitors on AA 2024-T3 assessed by electrochemical methods, Surf. Interface Anal. 47 (2015) 1029–1039. https://doi.org/10.1002/sia.5810.

[8] A.L.R. Silva, M.D.M.C. Ribeiro, Energetic , structural and tautomeric analysis of 2-mercaptobenzimidazole: an experimental and computational approach, J. Therm. Anal. Calorim. 129 (2017) 1679–1688.

[9] E. Milanova, S. Ellis, B. Sitholé, Aquatic toxicity and solution stability of two organic corrosion inhibitors: 2-mercaptobenzothiazole and 1,2,3-benzotriazole, Nord. Pulp Pap. Res. J. 16 (2001) 215–218. https://doi.org/10.3183/npprj-2001-16-03-p215-218.

[10] X. Wu, F. Wiame, V. Maurice, P. Marcus, Adsorption and thermal stability of 2-mercaptobenzothiazole corrosion inhibitor on metallic and pre-oxidized Cu(1 1 1) model surfaces, Appl. Surf. Sci. 508 (2020) 145132.

[11] Y.S. Tan, M.P. Srinivasan, S.O. Pehkonen, S.Y.M. Chooi, Self-assembled organic thin films on electroplated copper for prevention of corrosion, J. Vac. Sci. Technol. Vac. Surf. Films. 22 (2004) 1917–1925.

[12] M. Finšgar, D. Kek Merl, An electrochemical, long-term immersion, and XPS study of 2-mercaptobenzothiazole as a copper corrosion inhibitor in chloride solution, Corros. Sci. 83 (2014) 164–175.

[13] R. Woods, G.A. Hope, K. Watling, A SERS spectroelectrochemical investigation of the interaction of 2-mercaptobenzothiazole with copper , silver and gold surfaces, J. Appl. Electrochem. 30 (2000) 1209–1222.

[14] D. Chadwick, T. Hashemi, Electron spectroscopy of corrosion inhibitors: Surface films formed by 2-mercaptobenzothiazole and 2-mercaptobenzimidazole on copper, Surf. Sci. 89 (1979) 649–659.

[15] C.J. Lee, S.Y. Lee, M.R. Karim, M.S. Lee, Comparison of the adsorption orientation for 2-mercaptobenzothiazole and 2-mercaptobenzoxazole by SERS spectroscopy, Spectrochim. Acta Part A. 68 (2007) 1313–1319.
[16] R.K. Shervedani, A. Hatefi-mehrjardi, M.K. Babadi, Comparative electrochemical study of self-assembled monolayers of 2-mercaptobenzimidazole formed on polycrystalline gold electrode, Electrochimica Acta. 52 (2007) 7051–7060.
[17] X. Wu, F. Wiame, V. Maurice, P. Marcus, 2-Mercaptobenzothiazole corrosion inhibitor deposited at ultra-low pressure on model copper surfaces, Corros. Sci. 166 (2020) 108464.
[18] X. Wu, F. Wiame, V. Maurice, P. Marcus, Effects of water vapour on 2-mercaptobenzothiazole corrosion inhibitor films deposited on copper, Corros. Sci. 189 (2021) 109565.
[19] J.A. Ramírez-Cano, L. Veleva, Direct measurement of the adsorption kinetics of 2-mercaptobenzothiazole on a microcrystalline copper surface, Rev. Metal. 52 (2016).
[20] Y.I. Kuznetsov, M.O. Agafonkina, N.P. Andreeva, D.B. Vershok, Adsorption of 2-mercaptobenzthiazole on copper and MNZh-5-1 alloy and their protection from corrosion in aqueous solutions, Int. J. Corros. Scale Inhib. 9 (2020) 344–361.
[21] L.P. Kazansky, I.A. Selyaninov, Y.I. Kuznetsov, Adsorption of 2-mercaptobenzothiazole on copper surface from phosphate solutions, Appl. Surf. Sci. 258 (2012) 6807–6813.
[22] I.A. Arkhipushkin, Yu.E. Pronin, S.S. Vesely, L.P. Kazansky, Electrochemical and XPS study of 2-mercaptobenzothiazole nanolayers on zinc and copper surface, Int. J. Corros. Scale Inhib. 3 (2014) 078–088.
[23] F. Chiter, D. Costa, V. Maurice, P. Marcus, DFT investigation of 2-mercaptobenzothiazole adsorption on model oxidized copper surfaces and relationship with corrosion inhibition, Appl. Surf. Sci. 537 (2021) 147802. https://doi.org/10.1016/j.apsusc.2020.147802.
[24] L. Carbonell, C.M. Whelan, M. Kinsella, K. Maex, A thermal stability study of alkane and aromatic thiolate self-assembled monolayers on copper surfaces, Superlattices Microstruct. 36 (2004) 149–160.
[25] F. Caprioli, F. Decker, A.G. Marrani, M. Beccari, V. Di Castro, Copper protection by self-assembled monolayers of aromatic thiols in alkaline solutions, Phys. Chem. Chem. Phys. 12 (2010) 9230–9238. https://doi.org/10.1039/b925063h.
[26] K. Mansikkamäki, U. Haapanen, C. Johans, K. Kontturi, M. Valden, Adsorption of Benzotriazole on the Surface of Copper Alloys Studied by SECM and XPS, J. Electrochem. Soc. 153 (2006) B311–B318.
[27] M. Finšgar, 2-phenylimidazole corrosion inhibitor on copper: An XPS and ToF-SIMS surface analytical study, Coatings. 11 (2021).
[28] E. McCafferty, J.P. Wightman, Determination of the Concentration of Surface Hydroxyl Groups on Metal Oxide Films by a Quantitative XPS Method, Surf. Interface Anal. 26 (1998) 549–564.
[29] S. Tanuma, C.J. Powell, D.R. Penn, Calculations of electron inelastic mean free paths. IX. Data for 41 elemental solids over the 50 eV to 30 keV range, Surf. Interface Anal. 43 (2011) 689–713. https://doi.org/10.1002/sia.3522.
[30] G. Kresse, J. Furthmüller, Efficiency of ab-initio total energy calculations for metals and semiconductors using a plane-wave basis set, Comput. Mater. Sci. 6 (1996) 15–50. https://doi.org/10.1016/0927-0256(96)00008-0.
[31] G. Kresse, J. Hafner, *Ab initio* molecular-dynamics simulation of the liquid-metal–amorphous-semiconductor transition in germanium, Phys. Rev. B. 49 (1994) 14251–14269. https://doi.org/10.1103/PhysRevB.49.14251.
[32] G. Kresse, D. Joubert, From ultrasoft pseudopotentials to the projector augmented-wave method, Phys. Rev. B. 59 (1999) 1758–1775. https://doi.org/10.1103/PhysRevB.59.1758.
[33] J.P. Perdew, J.A. Chevary, S.H. Vosko, K.A. Jackson, M.R. Pederson, D.J. Singh, C. Fiolhais, Atoms, molecules, solids, and surfaces: Applications of the generalized gradient approximation for

exchange and correlation, Phys. Rev. B. 46 (1992) 6671–6687. https://doi.org/10.1103/PhysRevB.46.6671.
[34] J.P. Perdew, K. Burke, M. Ernzerhof, Generalized Gradient Approximation Made Simple, Phys. Rev. Lett. 77 (1996) 3865–3868. https://doi.org/10.1103/PhysRevLett.77.3865.
[35] M. Methfessel, A.T. Paxton, High-precision sampling for Brillouin-zone integration in metals, Phys. Rev. B. 40 (1989) 3616–3621. https://doi.org/10.1103/PhysRevB.40.3616.
[36] M. Dion, H. Rydberg, E. Schroder, D. Langreth, B. Lundqvist, Van der Waals density functional for general geometries, Phys. Rev. Lett. 92 (2004). https://doi.org/10.1103/PhysRevLett.92.246401.
[37] J. Klimeš, A. Michaelides, Perspective: Advances and challenges in treating van der Waals dispersion forces in density functional theory, J. Chem. Phys. 137 (2012) 120901. https://doi.org/10.1063/1.4754130.
[38] J. Klimeš, D.R. Bowler, A. Michaelides, Chemical accuracy for the van der Waals density functional, J. Phys. Condens. Matter. 22 (2010) 022201. https://doi.org/10.1088/0953-8984/22/2/022201.
[39] J. Klimeš, D.R. Bowler, A. Michaelides, Van der Waals density functionals applied to solids, Phys. Rev. B. 83 (2011) 195131. https://doi.org/10.1103/PhysRevB.83.195131.
[40] F. Chiter, D. Costa, V. Maurice, P. Marcus, DFT-Based Cu(111)||Cu_2O(111) Model for Copper Metal Covered by Ultrathin Copper Oxide: Structure, Electronic Properties, and Reactivity, J. Phys. Chem. C. 124 (2020) 17048–17057. https://doi.org/10.1021/acs.jpcc.0c04453.
[41] V.S. Dilimon, J. Denayer, J. Delhalle, Z. Mekhalif, Electrochemical and spectroscopic study of the self-assembling mechanism of normal and chelating alkanethiols on copper, Langmuir. 28 (2012) 6857–6865. https://doi.org/10.1021/la300021g.
[42] Y. Wang, J. Im, J.W. Soares, D.M. Steeves, J.E. Whitten, Thiol Adsorption on and Reduction of Copper Oxide Particles and Surfaces, Langmuir. 32 (2016) 3848–3857.
[43] X. Wu, F. Wiame, V. Maurice, P. Marcus, 2-Mercaptobenzothiazole corrosion inhibitor deposited at ultra-low pressure on model copper surfaces, Corros. Sci. 166:108464 (2020).
[44] X. Wu, F. Wiame, V. Maurice, P. Marcus, Molecular scale insights into interaction mechanisms between organic inhibitor film and copper, Npj Mater. Degrad. 5 (2021).
[45] Y. Yang, A.J. Wikieł, L.T. Dall'Agnol, P. Eloy, M.J. Genet, J.J.G. Moura, W. Sand, C.C. Dupont-Gillain, P.G. Rouxhet, Proteins dominate in the surface layers formed on materials exposed to extracellular polymeric substances from bacterial cultures, Biofouling. 32 (2016) 95–108. https://doi.org/10.1080/08927014.2015.1114609.
[46] N.S. McIntyre, M.G. Cook, X-Ray Photoelectron Studies on Some Oxides and Hydroxides of Cobalt, Nickel and Copper, Anal. Chem. 47 (1975) 2208–2213.
[47] J.C. Klein, C.P. Li, D.M. Hercules, F. James, Decomposition of Copper Compounds in X-Ray Photoelectron Spectrometers, Appl. Spectrosc. 38 (1984) 729–734.
[48] G. Deroubaix, P. Marcus, X-Ray Photoelectron Spectroscopy Analysis of Copper and Zinc Oxides and Sulphides, Surf. Interface Anal. 18 (1992) 39–46.
[49] B.E.T. Bautista, A.J. Wikiel, L. Datsenko, M. Vera, W. Sand, A. Seyeux, S. Zanna, I. Frateur, P. Marcus, Influence of extracellular polymeric substances (EPS) from Pseudomonas NCIMB 2021 on the corrosion behaviour of 70Cu-30Ni alloy in seawater, J. Electroanal. Chem. Interfacial Electrochem. 737 (2015) 184–197.
[50] R. Procaccini, W.H. Schreiner, M. Vázquez, S. Ceré, Surface study of films formed on copper and brass at open circuit potential, Appl. Surf. Sci. 268 (2013) 171–178. https://doi.org/10.1016/j.apsusc.2012.12.050.
[51] P.M. Natishan, W.E. O'Grady, Chloride Ion Interactions with Oxide-Covered Aluminum Leading to Pitting Corrosion: A Review, J. Electrochem. Soc. 161 (2014) C421–C432. https://doi.org/10.1149/2.1011409jes.

[52] E. Vernack, D. Costa, P. Tingaut, P. Marcus, DFT studies of 2-mercaptobenzothiazole and 2-mercaptobenzimidazole as corrosion inhibitors for copper, Corros. Sci. 174 (2020) 108840. https://doi.org/10.1016/j.corsci.2020.108840.
[53] I. a Arkhipushkin, P.Y. E, L.P. Kazansky, Electrochemical and XPS study of adsorption of 2-mercaptobenzothiazole on copper , zinc and brass surface ., (2014) 40.
[54] Y.S. Tan, M.P. Srinivasan, S.O. Pehkonen, S.Y.M. Chooi, Self-assembled organic thin films on electroplated copper for prevention of corrosion, J. Vac. Sci. Technol. 22 (2004) 1917–1925.
[55] S.W. Goh, A.N. Buckley, B. Gong, R. Woods, R.N. Lamb, L.J. Fan, Y. wen Yang, Thiolate layers on metal sulfides characterised by XPS, ToF-SIMS and NEXAFS spectroscopy, Miner. Eng. 21 (2008) 1026–1037.
[56] F. Chiter, D. Costa, V. Maurice, P. Marcus, Corrosion inhibition of locally de-passivated surfaces by DFT study of 2-mercaptobenzothiazole on copper, Npj Mater. Degrad. 5 (2021) 52. https://doi.org/10.1038/s41529-021-00198-x.
[57] F. Chiter, D. Costa, V. Maurice, P. Marcus, Chemical interaction, self-ordering and corrosion inhibition properties of 2-mercaptobenzothiazole monolayers: DFT atomistic modeling on metallic copper, Corros. Sci. 209 (2022) 110658. https://doi.org/10.1016/j.corsci.2022.110658.
[58] J.-H. Jhang, E.I. Altman, Water chemistry on two-dimensional silicates studied by density functional theory and temperature-programmed desorption, Surf. Sci. 679 (2019) 99–109. https://doi.org/10.1016/j.susc.2018.08.026.
[59] Y. Liu, J. Chen, Y. Li, J. Zhang, D. Kang, First-principles study on the adsorption structure of water molecules on a pyrite (100) surface, Physicochem. Probl. Miner. Process. (2021). https://doi.org/10.37190/ppmp/133010.
[60] D. Gustinčič, A. Kokalj, DFT Study of Azole Corrosion Inhibitors on Cu2O Model of Oxidized Copper Surfaces: I. Molecule–Surface and Cl–Surface Bonding, Metals. 8 (2018) 310. https://doi.org/10.3390/met8050310.
[61] F. Chiter, D. Costa, V. Maurice, P. Marcus, DFT investigation of 2-mercaptobenzothiazole adsorption on model oxidized copper surfaces and relationship with corrosion inhibition, Appl. Surf. Sci. 537 (2021).
[62] A. Abdureyim, K.K. Okudaira, Y. Harada, S. Masuda, M. Aoki, K. Seki, Characterization of 4-mercaptohydrocynnamic acid self-assembled film on Au(111) by means of X-ray photoelectron spectroscopy, J. Electron Spectrosc. Relat. Phenom. 114–116 (2001) 371–374.

CRediT authorship contribution statement

Elea Vernack : investigation, validation, writing-original draft, writing-review and editing, visualization, Dominique Costa: validation, formal analysis, writing original draft, writing review and editing, supervision, Sandrine Zanna : methodology, validation, writing original draft, writing-review and editing, Antoine Seyeux : methodology, validation, writing-review and editing, Fatah Chiter : investigation, validation, writing-original draft, visualization, Philippe Tingaut : funding acquisition, Philippe Marcus: conceptualization, writing-review and editing, project administation, funding acquisition

Declaration of Competing Interest

☒ The authors declare that they have no known competing financial interests or personal relationships that could have appeared to influence the work reported in this paper.

☐The authors declare the following financial interests/personal relationships which may be considered as potential competing interests:

Highlights

- MBT adsorbs on Cu immersed in water and forms multilayers with thicknesses of 2.3 to 3.2 nm
- Adsorbed MBT inhibits the copper oxide growth, Cl adsorption and copper dissolution in NaCl.
- The first MBT layer close to the substrate is bonded to copper via the two S atoms oriented towards the surface
- Water is present in the organic film in a ratio H_2O/MBT = 0.28
- Water in the organic film has a determinant role in molecule orientation, as shown by DFT calculations
- A fraction of MBT is adsorbed on metallic copper, healing some depassivated areas